B

BEACH

Charles W. Finkl
Department of Geosciences, Florida Atlantic University, Boca Raton, FL, USA
The Coastal Education and Research Foundation, Coconut Creek, FL, USA

Synonyms

Bank; Beachfront; Coast; Lakeshore; Lakeside; Littoral; Margin; Oceanfront; Seaboard; Seafront; Seashore; Seaside; Shingle; Shore; Strand; Waterfront

Definition

In the most rudimentary sense, a beach may be considered a shore (see Coasts) covered by sand (e.g., Shepard, 1973), gravel (e.g., Carter and Orford, 1984; Jennings and Shulmeister, 2002), or larger rock fragments (but lacking bare rock surfaces). More specifically, Jackson (1997) defines a beach as a relatively thick and transitory accumulation of loose waterborne materials that are mostly well-sorted sand and pebbles, but contains admixtures of mud, cobbles, boulders, smoothed rock, and shell fragments. The term was originally used in a scientific sense to designate loose waterworn shingle or pebbles on English shores (Johnson, 1919). Today, beaches are defined in a wider geomorphological sense as having subaerial and submarine components that are systematically interrelated. The beach system includes the dry (subaerial) beach, the wet beach (swash or intertidal zone), the surf zone, and the nearshore zone lying beyond the breakers (Short, 2006). Mostly the nearshore zone is defined as the area beginning from the low-water line extending seaward. The surf zone is part of the nearshore zone. The subaerial beach has a gentle seaward slope, typically with a concave profile, and extends from the low-water mark landward to a place where there is a change in material or physiography (such as a dune, bluff, or cliff, or even a seawall) or to the line of permanent vegetation marked by the limit of highest storm waves or surge. If the area beginning from the low-water line is regarded, the profile is not concave when looking to a beach with a certain tidal range. The dry beach is concave, but at low water when including the wet beach, the morphology switches from a concave beach (dry part) to a convex beach (wet part). Nearshore bars and troughs (in the subtidal domain) are often present in the surf zone, but are obscured by waves and surf, as is the always submerged nearshore zone (Short, 2006). Beach morphology refers to the shape of the beach, surf, and nearshore zone. The beach per se contains numerous morphological–processual subunits such as berms, storm ridges (e.g., Zenkovich, 1967; Pethick, 1984; Komar, 1998; Davis and FitzGerald, 2004), cusps, beach face, shoreface (e.g., Swift et al., 1985), plunge step (Davis and Fox, 1971), scarp, etc.

Related features include beach plains, beach ridges, and beachrock. Beach plains are level or gently undulating areas formed by closely spaced successive embankments of wave-deposited materials added to a prograding shoreline (Jackson, 1997). Beach ridges are low mounds of beach or beach-and-dune materials (sand, gravel, shingle) accumulated by waves on the backshore beyond the present limit of storm waves or ordinary tides. Beach ridges are roughly parallel to the shoreline and mark prior positions of an advancing shoreline (Jackson, 1997). Beachrock is a friable to well-cemented sedimentary rock formed in the intertidal zone in a tropical or subtropical region. Beachrock formations, which slope gently seaward on the beach face, consist of sand or gravel (detrital and skeletal) cemented with calcium carbonate.

J. Harff et al. (eds.), *Encyclopedia of Marine Geosciences*, DOI 10.1007/978-94-007-6238-1,

Etymology and usage

According to Merriam-Webster (1994), the first known use of the term beach was perhaps in 1535. The term beach was used to describe "loose, water-worn pebbles of the seashore," probably from Old English bæce, bece "stream," from Proto-Germanic *bakiz. Extended to loose, pebbly shores (1590s), and in dialect around Sussex and Kent, beach still has the meaning "pebbles worn by the waves." French grève shows the same evolution (http://www.etymonline.com/index.php?term=beach). Thus, early on the term *beach* did not refer to the expanse of sand normally thought of today. Expansion of term to cover the whole shore in the late sixteenth century may have been related to a popular misunderstanding of the "pebbles" connotation of "beach" in phrases such as "walk on the beach" (http://www.word-detective.com/2007/12/strand-beach/).

Geographic occurrence

Beaches are characteristic of almost all coasts where sediments accumulate alongshore. Sandy beaches occur in all latitudes where there are waves, appropriate types of sediments that are available for accumulation, and a favorable littoral geomorphology (e.g., Davies, 1980; Swift et al., 1985; Pilkey, 2003). Long straight beaches tend to occur along gently seaward-sloping continental shelves with abundant sediment supply, whereas curved beaches in coastal embayments are typically associated with steep continental shelves and a limited sediment supply (Masselink et al., 2011). Although most commonly associated with sedimentary coasts such as occur on barrier islands, for example, beach–dune systems may be quite extensive as major coastal features. It is estimated by various researchers that beaches occur along about a third of the world's coastline (Bird, 1984; Bird and Schwartz, 1985; van der Maarel, 1993), depending on the definitions used for compound coasts. Some coasts, for example, may be dominantly cliffy or rocky, but at the same time they contain beaches in front of the cliffs or between rocky promontories (Figure 1). That is to say, beaches may be small disjunctive pocket accumulations along rocky coasts or they may be the dominant coastal type. Australia, for example, has some 11,761 dominant beaches that make up half of the 30,000-km-long coast (Short and Farmer, 2012). Most Australian beaches, like many others throughout the world, are bordered by some kind of natural feature such as a dune field, cliff, headland, rocks, coral reef, or inlet. According to Dolan et al. (1972), 33 % of the North American shoreline is beach, which further breaks down to 23 % barrier-beach islands, 8 % pocket beaches, and 2 % associated with rock headlands. Of the 19,550-km-long shoreline of the contiguous USA, the US Army Corps of Engineers (COE, 1984) estimates that about 76,100 km (i.e., excluding Alaska, Hawaii, Puerto Rico, and US territories) is beach.

Some of the longest beaches in the world include, for example, Brazil's Praia do Cassino Beach (over 250 km

Beach, Figure 1 Carbonate beach on Long Island, Bahamas, showing biogenic carbonate sand derived from shells and coral reef materials that have been comminuted by wave action to form sand-sized grains. Note the soft pink color of the sand seaward of the wetted perimeter. The coral-rich beach sand contains admixtures of species of Foraminifera or forams (microscopic animals with bright red shells), making these pink beaches some of the best in the world. These beaches, bounded by eolianite headlands, occur on the open Atlantic Ocean side of the island and are also well known on Harbour Island near Eleuthera (Photo: C.W. Finkl).

long), India's Cox's Bazar (about 240 km long), Texas' Padre Island (about 210 km long), Australia's Coorong Beach (194 km), New Zealand's Ninety Mile Beach (each about 145 km long), Mexico's Playa Novillero (about 80 km long), and America's Virginia Beach (about 55 km long).

Grain size, shape, chemical composition, and color

Beaches are the product of wave-deposited sediment, but the materials comprising the beach have an almost unlimited range in size, shape, and composition. In practice, however, each beach area has a particular texture and composition with great variation occurring from place to place. Most beaches are sandy (composed predominantly of sand-sized grains, according to the Udden-Wentworth scale), but the term also includes shingle, gravel (pebbles and cobbles), and boulders that are deposited between the upper swash limit and wave base (e.g., Hardisty, 1990; Short and Woodroffe, 2009). Coarse-grained (cobble, boulder) beaches are prevalent in high latitudes and typify many coastal segments in Canada and the southern Baltic Sea coastline, for example, where glacial materials and bedrock are eroded by coastal processes. Coarse-grained beaches and barriers may also occur along many high-energy coasts, as seen along the west coast of North America, and in low latitudes where they are composed of shell or coral fragments (Figure 2).

Very fine-grained (high percentage of silt and clay) beaches may exceptionally occur under specialized conditions where there is an abundance of fine-grained sediments deposited by wave action as, for example, along the Red Sea and in the vicinity of large deltas and estuaries. A well-known example of a muddy coast with a potential for muddy "beaches" (mud flats) is provided by Anthony et al. (2010) for the 1,500-km-long coast of South America between the Amazon and the Orinoco river mouths. Ephemeral mud "beaches" also occur around mud-lump islands of the Mississippi Delta (Morgan et al. 1963). Similar "beaches" occur along the deltaic plains of the Brazos and Colorado rivers of the Texas coast and the eastern shore of Virginia (Davis, 1978).

Beaches tend to be comprised of well-sorted and generally rounded grains. Exceptions include disk, blade, and roller shapes that are so characteristic of gravel beaches where the larger clasts slide over sand and fine gravel (Pilkey et al., 2011). Biogenic beach gravels are also rather common and may comprise the entire beach sediment, as along coral reef beaches, or may be mixed with sand (cf. Figures 1 and 2). The abundance of biogenic debris (shell, algae, coral fragments) on beaches reflects the provenance of materials and the processes acting on the beach to produce a range of irregular shapes such as the pure *Acropora* coral stick beaches (Davis, 1978).

The composition of beach sediments depends on initial materials where terrigenous (or terrestrial, derived from the erosion of other rocks on land), volcanic (directly derived from volcanic activity and volcanic rocks), and biogenic (composed of shells and skeletons of dead marine organisms) lithologies contribute to the clastic pool (Pilkey et al., 2011). Siliciclastic (quartzose) beaches

Beach, Figure 2 Coarse-grained carbonate beach composed of shell hash on Captiva Island, southwest coast of the Florida Peninsula, USA, facing the Gulf of Mexico. Note the cuspate planform of the beach and a series of beach ridges containing shell fragments heaped up by wave action and swash (Photo: C.W. Finkl).

Beach, Figure 3 Siliciclastic beach sands on Amagansett Beach, Long Island, New York, USA, showing a reflective morphodynamic beach state. As swash runs up the steep beach face, it carries sand grains that overtop the berm to the back beach area. Interdigitating swash marks on the berm mark the landward most transport of sand grains that are dominantly quartz but which may contain minor admixtures of biogenic (shell) fragments and organic matter (Photo: C.W. Finkl).

tend to be more common in middle and high latitudes (Figure 3), whereas carbonates (aragonite and calcite) dominate tropical and subtropical zones. Although a small feldspar fraction is usually present in terrigenous sands, those few beaches that are rich in feldspar tend to be close to the source rock from which the feldspar is derived, such as glacial deposits derived from shield (cratonic) areas containing feldspar-rich granites and gneisses. Beach sands derived from granitic source areas sometimes contain heavy minerals (density > 2.9 g cm^3) that tend to be concentrated in the swash zone by the placering effect to form dark-colored streaks that are sorted out from the rest of the lighter-colored grains.

Beach color is determined by grain size and mineralogical composition so that silicates (derived from igneous granitic rocks, metamorphic rocks such as gneisses and schists, and preexisting sandstones) impart a light color to beaches (Figure 3), whereas more mafic compositions imbue black (Figure 4) to dark gray to dark green colors in fragments of fine-grained rocks such as metamorphic slates or volcanic ricks such as andesite and basalt (Pilkey et al., 2011). The inherent color of the beach's grains does not always determine beach color because grains may be stained by iron oxides, tannic acids, or microorganisms that may produce distinctly red, yellow, or green beaches, for example.

Types of beaches

Because beaches occur in all climatic zones, there are some obvious morphological differences related to severe conditions. In very high latitudes, for example, the water is frozen but for a few weeks when beaches may be affected by waves (Davis, 1978) and consequently beach morphology and texture is somewhat different from those in low latitudes. Beaches in arid climates depend almost solely on wave action to provide sediment from the bedrock coast to form a beach. The best developed beaches are associated with low-lying coasts where large quantities of sediment are available. Beach development requires an abundant sediment supply to produce characteristic morphologies and environmental zonations (Masselink et al., 2011).

The term *beach type* refers to the dominant nature of a beach based on tidal, wave, and current regimes, spatio-temporal extent of the nearshore zone, morphodynamics (beach width, shape, and processes) of the surf zone including bars and troughs, and the subaerial beach (Short, 1993). Irrespective of the specific beach type, most beaches contain several morphogenetic zones: (1) the backshore (nearly horizontal to gently landward-sloping area called the berm), (2) inner swash zone (upper limit of swash to the shoreline), (3) surf zone (from the shoreline to where waves break, the breaker zone), (4) nearshore zone (from the breaker zone, commonly with sandbars, to the wave base), and (5) wave base (depth where waves begin to interact with the seabed to transport sand to the beach and seaward to where sand is transported by large waves that cause beach erosion) (Davis, 1978; Short and Woodroffe, 2009). These zones are greatly variable, depending on the processes and materials that affect

Beach, Figure 4 Black sand beach composed of basaltic grains on the south coast of Iceland west of the Dyrhólaey promontory (headland or cape), near Vik. The mafic composition of the basaltic grains does not make the clasts particularly durable, and they are worn down by wave and surge action to finer-grained particles, as seen in the reticulate pattern on this extremely wide berm and beach plain where there are darker-colored coarse-grained ridges and lighter-colored finer-grained flats. This black basaltic beach and beach plain front a large sandur plain (Photo: C.W. Finkl).

beach type. In addition to these major zonations of beach environments, there are numerous smaller, but important, morphological features such as the plunge step (Davis and Fox, 1971), which is a small and commonly subtle shore-parallel depression in the foreshore that is caused by the final plunge of waves as they break for the last time before surging up the beach face (Davis, 1978).

Classification of beaches

Many factors need to be considered in the classification of beaches (e.g., Finkl, 2004) as they are among the most dynamic features on earth, but even so they retain certain overriding characteristics that facilitate generalization and categorization. The overall gradient of the beach and nearshore influences the amount of wave energy that reaches the beach, giving it its configuration. Beach materials, slope, and exposure interact with waves to produce the morphodynamic beach state that is constantly adjusting to new environmental conditions. Although beaches are one of the most dynamic morphosystems on earth (literally changing every day), they exhibit a range of characteristic morphologies that have been intensively studied in Australia. The analysis of Australian beach characteristics and shoreface dynamics (e.g., Short, 1993; Short, 1999) has led to a beach classification system that is now used internationally.

According to the classification scheme for Australian beaches (see discussion in Short and Woodroffe, 2009), there are 15 major beach types that are derived from three major beach systems: wave dominated, tide modified, and tide dominated. An overview of the beaches of Australia, which occupy half the 29,900-km-long coast (including Tasmania), is provided by Short (2006) in his discussion of the roles of waves, sediment, and tide range that contribute to beach type, particularly through the dimensionless fall velocity and relative tide range. Short's comprehensive study of Australian beach types includes descriptions of their regional distribution, together with the occurrence of rip currents, multibar beach systems, and the influence of geological inheritance and marine biota, a natural progression of comprehensive observational collages and models stemming from seminal works (e.g., Wright and Short, 1984) commonly referred to as the "Australian Beach Model" (Short, 2006).

Recognition of the 15 beach types occurring around the Australian coast provides a basis for identifying similar wave–tide–sediment environments throughout the world and classification of many of the world's beaches. Although applied internationally, the Australian Beach Model is not universal because it does not include tide-modified beaches exposed to higher ocean swell and storm seas, resulting in similar though higher-energy beaches, gravel, and cobble beaches (few occur in Australia), nor ice-affected beaches (because they do not occur in Australia). Nevertheless, this system finds wide application throughout the world as, for example, in the classification and study of Florida east coast beaches (e.g., Benedet et al., 2004), eastern Brazil (e.g., Klein

and Menezes, 2001), India (Saravanan et al., 2011), Portugal (e.g., Coelho, Lopes, and Freitas, 2009), France (Sabatier et al., 2009), and so on.

Artificial beaches

When beaches erode along developed shorelines, they are often replenished by sand dredged from offshore and pumped back onto the shore as remediation. Efforts are made to ensure that the dredged sediment closely approximates the nature (size, shape, density, durability, composition, and color) of native beach sands onshore (e.g., Finkl and Walker, 2005). Replenished beaches are engineered to approximate natural morphodynamic beach states so that they perform as sacrificial sand deposits over desired time frames. Some artificial beaches may erode very quickly if impacted by storms and thus fall short of the design life, while others, having greater durability, may exceed the design life, as in the case of Miami Beach, Florida, which has the longest half-life of any renourished beach in America (e.g., Finkl and Walker, 2005). The practice of building artificial beaches, as a soft-engineering shore protection measure, is now so widespread worldwide that many renourished beaches are perceived as natural formations. The practice is, however, not without environmental concerns as borrow sources do not always closely match native beach sands to cause unwanted impacts in the coastal zone (e.g., Bonne, 2010).

Summary

Beaches occur in all latitudes, from tropical to polar regions, and lie on the interface between land and water to form ocean, bay (sound, estuary), and river beaches. They are mostly composed of sand (silicates and carbonates), but there is great compositional and morphological variation between sites. Beaches have great economic and environmental value, serving as tourist destinations and providing habitat as well as buffering impacts from storm waves and surges. Some beaches are artificial, and although their placement is controversial among certain special interest groups, their benefits generally outweigh disadvantages when properly engineered and placed. The morphodynamic classification of beach state finds global application, provides greater understanding of Beach Processes, and contributes to beach safety education programs and surf life saving to reduce public risk.

Bibliography

Anthony, E. J., Gardel, A., Gratiot, N., Proisy, C., Allison, M. A., Dolique, F., and Fromard, F., 2010. The Amazon-influenced muddy coast of South America: a review of mud-bank-shoreline interactions. *Earth-Science Reviews*, **103**(2010), 99–121.

Benedet, L., Finkl, C. W., and Klein, A. H. F., 2004. Morphodynamic classification of beaches on the Atlantic coast of Florida: geographical variability of beach types, beach safety, and Coastal Hazards. *Journal of Coastal Research* (Special Issue No. 39), 360–365.

Bird, E. C. F., 1984. *Coasts: An Introduction to Coastal Geomorphology*. Oxford: Blackwell, 320 p.

Bird, E. C. F., and Schwartz, M. L. (eds.), 1985. *The World's Coastline*. New York: Van Nostrand Reinhold, 1071 p.

Bonne, W. M. I., 2010. European marine sand and gravel resources: evaluation and environmental impacts of extraction – an introduction. In Lancker, V. V.; Bonne, W., Uriarte, A., and Collins, M (eds.), *EUMARSAND: European Marine Sand and Gravel Resources. Journal of Coastal Research*, Special Issue #51, i–vi.

Carter, R. W. G., and Orford, J. D., 1984. Coarse clastic barrier beaches: a discussion of the distinctive dynamic and morphosedimentary characteristics. In Greenwood, B., and Davis, R. A. (eds.), *Hydrodynamics and Sedimentation in Wave-Dominated Coastal Environments. Marine Geology*, **60**, 377–389.

COE (Corps of Engineers), (1984). *Shore Protection Manual*. Vicksburg, MS: Coastal Engineering Research Center, 2 Vols. Available in electronic form: http://openlibrary.org/books/OL3001149M/Shore_protection_manual; and as the *Coastal Engineering Manual* at http://chl.erdc.usace.army.mil/cem

Coelho, C., Lopes, D., and Freitas, P., 2009. Morphodynamics classification of Areão Beach, Portugal. *Journal of Coastal Research*, (Special issue No. 56), 34–38.

Davies, J. L., 1980. *Geographical Variation in Coastal Development*. London: Longman, 204 p.

Davis, R. A., 1978. *Coastal Sedimentary Environments*. New York: Springer, 420 p.

Davis, R. A., and FitzGerald, D. M., 2004. *Beaches and Coasts*. Malden, MA: Blackwell, 419 p.

Davis, R. A., and Fox, W. T., 1971. *Beach and Nearshore Dynamics in Eastern Lake Michigan*. Kalamazoo, MI: Western Michigan University. Technical Report No. 4 (ONR Contract 388–092), 145 p.

Dolan, R., Hayden, B., Hornberger, G., Zieman, J., and Vincent, M., (1972). *Classification of the Coastal Environments of the World. Part I, The Americas.* Charlottesville, VA: University of Virginia. Technical Report No. 1 (ONR Contract 389–158), 13 p.

Finkl, C. W., 2004. Coastal classification: systematic approaches to consider in the development of a comprehensive scheme. *Journal of Coastal Research*, **20**(1), 166–213.

Finkl, C. W., and Walker, H. J., 2005. Beach nourishment. In Schwartz, M. (ed.), *The Encyclopedia of Coastal Science*. Dordrecht, The Netherlands: Kluwer Academic (now Springer), pp. 147–161.

Hardisty, J., 1990. *Beaches: Form and Processes*. London: Unwin Hyman, 324 p.

Jackson, J. A., 1997. Glossary of geology. Denver, Colorado: American Geological Institute, 769 p.

Jennings, R., and Shulmeister, J., 2002. A field based classification scheme for gravel beaches. *Marine Geology*, **186**(3–4), 211–228.

Johnson, D. W., 1919. Shore processes and shoreline development. New York: Wiley, 584 p.

Klein, A. H. F., and Menezes, J. T., 2001. Beach morphodynamic and profile sequence for a headland bay coast. *Journal of Coastal Research*, **17**, 812–835.

Komar, P. D., 1998. *Beach Processes and Sedimentation*. Upper Saddle River, NJ: Prentice Hall.

Masselink, G., Hughes, M. G., and Knight, J., 2011. *Introduction to Coastal Processes and Geomorphology*. London: Arnold.

Merriam-Webster, 1994. *Merriam-Webster's Dictionary of English Usage*. Springfield, MA: Merriam-Webster, 989 p.

Morgan, J. O., Coleman, J. M., and Gagliano, S. W., 1963. *Mudlumps at the Mouth of South Pass, Mississippi River; Sedimentology, Paleontology, Structures, Origin and Relation to Deltaic Processes*. Baton Rouge, LA: Louisiana State University Studies. Coastal Studies Series No. 10.

Pethick, J., 1984. *An Introduction to Coastal Geomorphology*. London: Edward Arnold, 260 p.

Pilkey, O. H., 2003. *A Celebration of the World's Barrier Islands*. New York: Columbia University, 309 p.

Pilkey, O. H., Neal, W. J., Kelley, J. T., and Cooper, A. G., 2011. *The World's Beaches*. Berkeley, CA: University of California Press, 283 p.
Sabatier, F., Anthony, E. J., Héquette, A., Suanez, S., Musereau, J., Ruz, M.-H., and Regnauld, H., 2009. Morphodynamics of beach/dune systems: examples from the coast of France. *Geomorphologie*, **1**(2009), 3–22.
Saravanan, S., Chandrasekar, N., Sheik Mujabar, P., and Hentry, C., 2011. An overview of beach morphodynamic classification along the beaches between Ovari and Kanyakumari, southern Tamil Nadu coast, India. *Physical Oceanography*, **21**(2), 57–71.
Shepard, F. P., 1973. *Submarine Geology*. New York: Harper and Row, 517 p.
Short, A. D., 1993. *Beaches of the New South Wales Coast: A Guide to the Nature, Characteristics, Surf and Safety*. Sydney, NSW: Australian Beach Safety and Management Program, 358 p.
Short, A. D., 1999. *Handbook of Beach and Shoreface Morphodynamics*. Chichester: Wiley, 379 p.
Short, A. D., 2006. Australian beach systems – nature and distribution. *Journal of Coastal Research*, **22**(1), 11–27.
Short, A. D., and Farmer, B., 2012. *101 Best Australian Beaches*. Sydney, NSW: NewSouth Publishing, 222 p.
Short, A. D., and Woodroffe, C. D., 2009. *The Coast of Australia*. Cambridge: Cambridge University Press, 288 p.
Swift, D. J. P., Niederoda, A. W., Vincent, C. E., and Hopkins, T. S., 1985. Barrier island evolution, middle Atlantic shelf, U.S.A. Part I: shoreface dynamics. *Marine Geology*, **63**, 331–361.
van der Maarel, E. (ed.), 1993. *Dry Coastal Ecosystems: Polar Regions and Europe*. Amsterdam, The Netherlands: Elsevier, Ecosystems of the World, Vol. 2A, 600 p.
Wright, L. D., and Short, A. D., 1984. Morphodynamic variability of surf zones and beaches: a synthesis. *Marine Geology*, **56**, 93–118.
Zenkovich, V. P., 1967. *Processes of Coastal Development*. Edinburgh: Oliver and Boyd, 73 p.

Cross-references

Beach Processes
Coastal Engineering
Dunes
Engineered Coasts
Integrated Coastal Zone Management
Placer Deposits
Reef Coasts
Sea Walls/Revetments
Sediment Transport Models
Shelf
Waves

BEACH PROCESSES

Charles W. Finkl
Department of Geosciences, Florida Atlantic University, Boca Raton, FL, USA
The Coastal Education and Research Foundation, Coconut Creek, FL, USA

Synonyms

Beach morphodynamics; Coastal processes; Cusp formation; Littoral processes; Surf zone processes

Definition

The term *beach processes* refers to the collection of processes that are responsible for the formation and maintenance of morphological features and materials that make up all facets of units comprising the beach per se. Because the beach has subaerial and submarine components, processes range from the effects of wind to waves, currents, and tides acting on sediment supply and redistribution to form beach types. Important processes include swash run-up and rundown, overtopping, infiltration into the beachface, step generation, bar formation, cusp development, and so on. Processes and materials interact in a dynamic manner in continual adjustment to changing environmental conditions associated with wind regimes, wave climates, tides, and extreme events such as storm surge and tsunamis.

Introduction

Beaches are complex systems that at first glance appear to be simple enough, sediment piled up along the shore. But, nothing could be farther from the truth as these dynamic systems have historically defied articulation and comprehension because of their continual short-term modification in terms of minutes to hours (e.g., Bascom, 1980; Carter, 1988). High-energy events can induce large-scale beach change that is immediately apparent to an observer. But, even during quiescent periods, the beach is continually changing; literally with every wave grains are moved about the beachface in laminar up- or downrush or by saltation on the berm. Over a longer decadal time frame, some beach materials in tropical and subtropical regions may become indurated by calcium carbonate to form beachrock that in turn provides long-term stability to the beach. Beach processes are similar in general but very different in detail, depending on the ambient energy conditions and materials present. Much is known about beach processes, but some exact modes of formation for some beach features such as beach cusps remain elusive (Guza and Inman, 1975; Komar, 1997; Davidson-Arnott, 2009; Pilkey et al., 2011).

The main agents that affect beaches include waves, tides, currents, and wind (on the dry backbeach area), all of which interact with the sediment to produce distinctive beach morphologies (e.g., Bascom, 1954; Pethick, 1984; Woodroffe, 2002; Davis and FitzGerald, 2004). Breaking waves obviously interact with the sediment, and their position along the beachface depends on tidal ranges and setup or surge. Currents produced by the waves are among the most important processes that change the beach. These important sediment-transporting currents include: (1) combined flow currents, (2) longshore currents, (3) rip currents, and (4) onshore-offshore (cross-shore) currents produced in the swash zone (Davis and FitzGerald, 2004).

Beaches contain noncohesive materials that accumulate in areas affected by wave action along the perimeter of a body of water (whether fresh, brackish, marine, or hypersaline). The material is commonly sand-sized grains

Beach Processes, Figure 1 Dissipative beach along the Oregon coast showing the low-gradient swash that moves up the beachface as laminar flow. Successive incursions of swash move up the beachface as hydraulic jumps until they lose forward momentum and infiltrate into the beach. The high beach groundwater table close to the surface allows swash to run up the beachface for long distances. Pebble and gravel-sized clasts are heaped farther up the beach by storm waves. The backbeach contains coarse-grained lag that has been winnowed by currents when setup temporarily superelevates sea-level during storms (Photo by C.W. Finkl).

(0.06–2.0 mm), but may range through gravel (2–60 mm), cobbles (60–200 mm), and boulders (over 200 mm). Figure 1 shows a gradation in grain size from fine sand on the beachface to cobbles in the backbeach area at the foot of a cliff along the Oregon coast. In very specialized environmental settings, some beaches contain fine-grained materials that are admixed with sand. Intertidal beaches permanently rich in mud (10–20 %) on wave-dominated coasts are, for example, extremely rare because of hydrodynamically controlled nondeposition of mud and lack of substantial nearby mud supplies (Anthony et al., 2011). Mud-rich beaches are generally found associated with high fine-grained discharge deltas such as the Amazon (Anthony and Dolique, 2004) and Mekong (Tamura et al., 2010).

The beach zone is typically subdivided into nearshore, foreshore, and backshore; boundaries between these zones are elastic, responding to cyclic migrations and geo-hydro-meteodynamic events (e.g., Davidson-Arnott, 2009). The nearshore is the submarine part of the beach that lies seaward of the low-tide limit in the region of shoaling waves. The foreshore extends from the low-tide limit to the high-tide upper swash limit that is often marked by a line of flotsam and jetsam. The backshore typically lies landward of the high-tide swash limit and exceptionally lies along the landward limit of storm surge that may include cliffs, dunes, or marshes. The crest of the backshore zone, above the uppermost limit of normal swash, is called the berm. A beach typically has one berm, but there may be several berms depending on cycles and severity of storminess (e.g., Hardisty, 1990; Short, 1999). The example of the Brazilian beach shown in Figure 2 contains a gently seaward-sloping foreshore, a wide berm, and a narrow backbeach fronting eroded dune fronts.

Study of beach processes

Beach processes are studied in many different ways, as, for example, in the field, in wave tanks, or by numerical simulation on computers (e.g., Hardisty, 1990; Dean and Dalrymple, 2002; Davidson-Arnott, 2005; Dingler, 2005). Whatever approach is used, it is necessary to be cognizant of morphodynamic features such as the cross-shore (equilibrium) profile, presence and interaction of rock alongshore as backbeach cliffs, promontories, beachface beachrock, tidal or subtidal hardgrounds, skerries, or coral reefs offshore. The nature of sedimentary materials that is available for beach processes to act upon, the alongshore supply of sediments, offshore biogenic supply of sediments, and thickness of unconsolidated sediments along the continental shelf are all important parameters that influence beach type (Pilkey et al., 2011). It is also not a matter of presence or absence of any of these features, but the degree to which they are present, or not. With so many cross feedback mechanisms, it is generally not possible to isolate discrete processes that do not interact with other processes or which are modified by different kinds of materials that they act upon.

Beach Processes, Figure 2 Intermediate beach morphotype on the coast of Santa Caterina, Brazil. A wide berm lies landward of a low-tide terrace with poorly developed ridges and runnels. Storm surges have nipped away the front of the backbeach dunes bringing dune sand back into the beach system. The maximum extent of inland penetration of swash is marked by the change in the color of the sand on the berm from darker yellow to cream colored on the backbeach (Photo by C.W. Finkl).

Beaches are thus complex processual systems that require much tenacity and expertise to tease out the secrets of beach formation and modification. In spite of the complexity involved, it is possible to outline some of the main processes that are responsible for major beach features. It is also perhaps worth mentioning at this point that it is not profitable to attempt discussion of beach processes without considering the morphological properties of beach features. The association of process and form (Hardisty, 1990) thus leads to appreciation of beach morphodynamics (e.g., Short, 2006), which includes the interaction between breaking waves, currents, rocky headland or submerged hardgrounds, and the sediments that compose the beach. Beaches are dynamic features where composition, morphology, and orientation are spatio-temporally variable as, for example, in the case of headland bay beaches that rotate between promontories (Klein et al., 2002; Short and Trembanis, 2004).

Small-scale beach processes

Waves and currents sort the sediment and move it alongshore and cross-shore. The concept of a "river of sand" is sometimes promoted, but it is a misnomer because there can be many interruptions to the alongshore sediment flow as in the case of capes, promontories (headlands), submarine canyons, deeply dredged inlets, or other engineering structures such as groins and jetties. Alongshore drift may be predominantly in one direction, but there can be seasonal reversals (e.g., during monsoons) or interruptions due to storms, making the concepts of gross and net sediment transport viable (Dean and Dalrymple, 2002). As a general rule in sandy environments, coarser materials remain closer to shore, but along high-energy coasts coarse materials may be heaped up on the beachface and berm. Below mobile surface sediments, bedrock platforms or consolidated materials slope gently seaward, serving as a foundation for the beach. Some beach sediments are heaped up on marine benches during storms and because they lie beyond normal waves and tidal cycles, they are referred to as *perched beaches* being the result of special extreme processes.

Beaches exist in a state of dynamic equilibrium with tides and waves. Storm waves tend to move the sand out to deeper water and flatten the beach cross-shore profile while less energetic waves in quiescent periods tend to move sediment shoreward to build up the beach. Some beaches retain sand that is trapped between headlands, while in other settings sand transits the beach by entering in one end and exiting in the other, somewhat in the context of a conveyor belt. The beach therefore exists when processes and materials balance each other over time (e.g., Dean and Dalrymple, 2002; Davis and FitzGerald, 2004).

The surf zone, the most dynamic part of the beach, extends from the breaker zone to the shore (Wright and Short, 1984). Waves theoretically break when the slope of the advancing face is steeper than 1:0.78 but may be closer to 1:1 based on field data. Waves typically start to interact with the seafloor when the water depth is about 75–80 % of the wave height (Bascom, 1980). Frictional

forces then slow the bottom part of the wave while the top continues to move at the same speed, eventually over reaching the slower moving wave base. Waves may break as spilling breakers on low-gradient slopes, as plunging waves on moderate gradients, or as surging waves on steep slopes. Breaking waves transform their potential energy into kinetic energy in the form of broken waves of translation, or wave bores that move shoreward as turbulent white water. Breaking waves dissipate most of their forward-moving energy, which is lost in turbulence. Turbulent flow is an important process because it stirs up large quantities of bottom sediment that will remain in suspension for variable amounts of time depending on the grain size, larger particles settling faster than smaller ones according to Stoke's law and measured in numerous ways in the lab and in the field. This entrained sediment is transported more or less parallel to the shore by the longshore current, which typically reaches from the shoreline through the breaker zone. Under high-energy conditions, breaking storm waves advance across the upper shoreface, sending surge and fast-moving swash up the beachface to erode the berm (Figure 3). Under these conditions when the surf zone temporarily moves shoreward due to increased water depths resulting from surge and setup, beach sands are entrained in cross-shore currents leaving a beach scarp cut into the berm. Beaches equilibrate to a morphodynamic state that is more in balance with quiescent conditions after the storm passes.

Beach Processes, Figure 3 Reflective beach type now adjusting to an intermediate morphotype after the passage of storm conditions along the Florida Atlantic coast near Palm Beach. During the high-energy storm conditions, sand was eroded from the berm forming a new steeper beachface than the more gently sloping one associated with the formerly wider beach. The beach scarp, now a hazard to beachgoers, will slump by uprush undercutting during high tides to form a new more gently seaward-sloping beachface (Photo by C.W. Finkl).

Saltation on the berm and backbeach

Once sandy particles are deposited on the berm, wind is the predominant force that moves them inland. Wave-deposited materials are dried by solar radiation, wind, and drainage prior to transport by wind from the berm to backbeach. Wind velocity controls the rate of sand transport, but spatio-temporal variation in sediment deposition depends on beach width (Pethick, 1984; Davidson-Arnott and Law, 1996).

Three main eolian processes transport sediment (Bagnold, 1941). Wind erosion of surface particles on the berm is initiated when air velocities reach about 4.5 m s^{-1}. Initial particle movement takes place as a rolling motion, termed traction or creep, where particles as large as small pebbles can be tracted by strong winds. About 20–25 % of wind erosion is by traction. When particles are lifted off the ground, becoming suspended in the air, and then return to the ground surface several centimeters downwind, the process is called saltation (Davis, 1985; Carter, 1988). Saltation on the dry berm accounts for 75–80 % of total sediment transport by wind, with beach sand ultimately ending up in dunes behind the beach (Cf. Figure 2). It provides momentum that drives the other two sand transport modes because when a falling particle strikes the berm surface, part of its impact force is transferred to another particle causing it to become airborne.

Swash run-up and rundown

When beachfaces are steep, waves can transit the shoreface without breaking, and when the broken wave reaches the base of the wet beach, it collapses and runs up the beachface as swash or uprush in the swash zone (e.g., Davis and FitzGerald, 2004). Under normal or quiescent wave conditions, the laminar-flow uprush stops near the top of the slope, with some of the water infiltrating the surface of the beachface per se and then percolating into the beach until it reaches the water table (Cf. Figure 1). If the water table is close to the surface, the remainder flows back down the beachface as backwash. If the water table does not lie close to the surface, the uprush may completely disappear into the beachface with no back flow. These actions produce a relatively steep seaward-sloping swash zone on the beachface, the slope of which can range from 1° to 20°. If waves approach the beach obliquely, and although sediment in this case is transported in a zigzag pattern across the

Beach Processes, Figure 4 Current ripples along the foreshore on a beach in Long Island Sound near Amagansett, Long Island, New York, USA. Shore-parallel ripples in this intertidal zone are developed on both sides (landward and seaward) of a hardground containing algal overgrowth. A hydraulic jump is visible in the swash seaward of the algae poking through the sand cover. The complexity of these small-scale beach processes is shown by superposition of fine-grained sand in a micro-delta deposited on top of the rippled sand bed, as noted by the lighter color of the sand splay and lack of closely spaced ripples. In addition to physical processes, beaches are modified by biological processes as, for example, seen here with mounds (that look like micro-volcanoes approximately 15 cm in diameter) produced by Atlantic jackknife clams (*Ensis directus*) (Photo by C.W. Finkl).

beachface, the net result is sediment transport in the direction of the waves. As sediment accumulates in a seaward-building swash zone, it constructs a berm, the nearly horizontal to slightly landward-dipping sand surface that merges with the backbeach. This is the so-called dry beach where most people sit or lay down when they go to the beach. The swash zone may contain small-scale features such as beach cusps, spaced about every 20–30 m apart, and which are thought to be produced by edge waves (Guza and Inman, 1975). On intertidal flat-lying parts of the foreshore, swash currents may produce various types of ripples. The ripples shown in Figure 4 are typical of many low-gradient intertidal beaches with fine-grained sediments, as seen on this beach on Long Island, New York, where the ripples formed by progressively dissipating swash currents during a falling tidal sequence.

Sheetwash, runoff channel, and sapping-seepage erosion

Rain-induced beach processes (Otvos, 1999) produce interesting minor features on beaches. Subtle features on sandy beach foreshores include swash grooves (braided scour marks), shore normal, flutes, dendritic rills, rhomboidal microrills, and box canyon valleys. These features are related to a range of processes such as water infiltration (in the infiltration zone) and percolation from the beach (in the effluent zone) at low tide or following a storm (e.g., Duncan, 1964; Davis, 1985; Komar, 1997), backwash deflection around obstacles (e.g., Otvos, 1964, 1965; Komar, 1997), backwash flow dissipating into the beach and emerging on the foreshore (Higgins, 1984), sheetwash and cross-beach channeled flow (Otvos, 1999), foreshore dissection by headward eroding box canyons and rill channels (Otvos, 1999), etc. Sheetwash, channeled surface flow, and fresh groundwater-driven spring sapping processes produce a wide range of micromorphodynamic features on the beachface and foreshore. Although appearing to be morphologically minor, these processes play an important subsidiary role in seasonal beach degradation and operate on most beaches of the world. These processes are significant in sediment redistribution on coasts with high rainfalls and wide beaches that are backed by permeable bluffs.

Plunge step formation

The plunge step occurs between the base of the foreshore and the top of the shoreface (Davis, 1985). Wave-dominated shorelines often show a sharp break in grain size at the plunge step where coarser clasts tend to accumulate. The plunge step marks a subtle decline in the foreshore profile that is produced by the final plunge (wave break) before a wave runs up the beachface (Pilkey et al., 2011). The last wave break converts potential energy into kinetic energy that is used up in turbulent flow.

Continual wave breaks in the same location alongshore suspends beach sediments that are transported by currents. The continuous turbulent action and cross-shore movement of sand grains creates a sedimentation deficit that produces the small alongshore trough. The penultimate forward movement of the wave thus moves up the beachface as laminar flow, often with several hydraulic jumps as successive waves break and send new swash on top of the preceding swash flow, in piggyback fashion. Bathers entering the surf are often surprised by the presence of the plunge step, especially when the water is murky, because it may be of decimeter scale, the deeper parts of the trough collecting organic debris that is unpleasant to walk through. The plunge step is best developed in low-tidal range beaches with a steep foreshore slope (Davis, 1985), such as commonly seen along Florida Atlantic coast beaches but is also common along gravel beaches. When setup is very high, the plunge step site may transfer up the beachface to the swash berm or even the storm berm. Direct measurement of step morphology is rare on account of the high-energy conditions localized along this zone.

Bar formation and migration

Surf zone currents transport sediment onshore, alongshore, and offshore to build (sand) wave-formed nearshore bars and troughs occupying the surf zone (e.g., Davis, 1985; Komar, 1997; Greenwood, 2005). Wave-formed bars occur as symmetrical or asymmetrical undulations along the upper shoreface profile in intertidal and subtidal environments (Greenwood, 2005). Barred profiles are in general associated with large values of wave steepness and wave height-to-grain size ratios and are associated with waning stages of shoaling and dissipation of wave energy (Wright et al., 1979; Greenwood, 2005). Bar formation has been related to a number of specific hypotheses that involve convergence of sediment transport, viz., (1) breakpoint hypotheses, (2) infragravity wave hypotheses, and (3) self-organization hypotheses. Wave breaking, for example, is thought to induce a seaward transport of sediment that is, respectively, entrained by roller or helical vortices under plunging or spilling breakers (e.g., Zhang, 1994). Alternatively, convergence of sediment at the breakpoint may be related to onshore transport associated with increasing asymmetry and skewness of high-frequency incident waves and offshore transport through setup-induced undertow (e.g., Thornton et al., 1996). Bar frequency of occurrence and geomorphic position may be produced by the interaction of sandy sediments with infragravity waves that are low frequency (greater 30 s period) waves produced by sets of higher and lower waves that are enhanced by wave breaking across the surf zone. These waves can be standing or progressive-produced as a result of energy dissipation during breaking and frequently related to groupiness (Roelvink and Broker, 1993; Reussink, 1998), amplitude modulation of the incident wave field. As a rule, the longer the infragravity wave period, the more widely spaced the bar(s).

Rip currents and channels

Rip currents are narrow, usually fast seaward-flowing currents that penetrate the surf zone, often in a rip channel that flows to deeper water. Rips are a mechanism for returning water back to the sea that piles up alongshore in setup (e.g., Pilkey et al., 2011; Leatherman, 2013). These fast-moving shore-perpendicular currents transport eroded beach sediment seaward to deep water during high seas. These fast-moving cross-shore currents often occur through gaps in offshore bars but are also caused by depressions in the beach, irregular bottom topography, obstructions in the surf zone such as rock outcrops or groins, or longshore currents in circulating cells (e.g., Pilkey et al., 2011). Rip currents, a major hazard to swimmers, are responsible for most beach rescues and drownings (Short, 1999; Leatherman, 2013). Edge waves, a form of infragravity wave (Guza and Inman, 1975; Reussink, 1998), influence the alongshore spacing of rip currents and channels, which are typically 200–300 m apart on open ocean beaches. Bars and troughs that form on the intertidal part of the beach are known as ridges and runnels, with sometimes as many as a dozen or more occurring on intertidal beaches with high tidal ranges. Individual bars may have their own swash zones and dry beach on the crests until they are covered by the rising tide.

Large-scale morphodynamic beach processes

Equilibrium beach (cross-shore) profiles are produced by steady wave forcing during seasonal cycles. Accretionary (summer) and erosional (winter) beach profiles are expressions of seasonal cycles of wave energy, as elucidated in the classic works of Shepard (1950) and Bascom (1954). Accretionary beaches, which are produced by swell waves with a low wave height (generally <1 m) and a period of 8–12 s, produce a wide and well-developed backbeach with a relatively narrow foreshore (e.g., Davis and FitzGerald, 2004).

Large storm events result in a disequilibrium profile where sand may be permanently lost to deep water (Dean and Dalrymple, 2002). Erosional or storm beaches, on the other hand, are temporary morphodynamic states that are characterized by a profile that is generally flat and featureless with a narrow or nonexistent backbeach (Shepard, 1950; Hallermeier, 1981). Most or all of the beach thus occur in the foreshore position (e.g., Davis and FitzGerald, 2004). Due to storms, waves are larger and more energetic in winter than summer. Long periods of stormy weather, such as El Niño winters, erode beaches to the underlying cobbles or bedrock and deposit sand far offshore in deep water, leaving the beach in disequilibrium, as seen, for example, along the California coast. The winter beach is denuded of sand by storm waves, leaving heavier cobbles behind as lag deposits. Wave-cut platforms underlying the mobile sediments are often

exposed during high-energy conditions. Summer wave conditions return sand back to the beach so that the summer beach is covered with a layer of sand that is moved south by alongshore currents and onshore by low-energy wave climate. Other researchers have noted associations between waves, breakers, and beach gradients – the relationship occurring because breaker type is a function of wave characteristics (Pethick, 1984). High values of the surf-scaling factor (e.g., Guza and Inman, 1975) are associated, for example, with wide flat beaches with spilling breakers, while low values are associated with steep narrow beaches and surging breakers (e.g., Wright et al., 1979; Wright et al., 1982). Although the relationship between wave steepness and beach gradient is pronounced, other variables such as the angle of the wave approach (e.g., Sonu and van Beek, 1971) and tides and longshore currents (e.g., Davis, 1985) may also be important.

Morphodynamic beach types

Beach morphotypes range through a sequence of process-form-materials systems between end points marked by low-energy systems with small beach-building waves to high-energy systems with large waves breaking across several hundred meters of surf zone (Wright and Short, 1984). Tides are an additional consideration in beach formation as they range from micro (<2 m), meso (2–4 m), macro (4–8 m), to mega tides (>8 m). Beaches are divided into the three basic morphodynamic types in order to accommodate tidal ranges, wave heights, and variations in grain size (sand to boulders), viz., wave dominated, tide modified, and tide dominated, based on the relative tide range (RTR) (Short, 2006). This process-based grouping of beach morphotypes, as initially conceived by Wright et al. (1982) and expanded to beaches around the Australian continent by Short (1999, 2006, 2012), provides a basis for cataloguing a range of beach processes associated with beaches in low latitude and mid-latitude. Ice-coast beach processes are not yet comprehensively included in the system. Some essential facets of the morphodynamic classification of beaches are briefly summarized here from Short (2012) and Short and Woodroffe (2009).

Wave-dominated beaches are characterized by a RTR tide range that is less than three times the average wave height (RTR < 3). These beaches occur in three morphodynamic states that are referred to as (1) reflective, (2) intermediate, and (3) dissipative.

Reflective beaches are the result of process-material interactions that are associated with lower waves (H < 0.5 m), longer wave periods, and coarser sediment. As a result of these process-form relationships, all coarse sand and cobble-boulder beaches exhibit a reflective beach state. Reflective beaches contain a relatively steep beachface (5–20°) that reflects backwash. Reflective beach processes do not produce a bar or surf zone.

Intermediate beaches are common along open coasts and are produced by moderate waves (H = 0.5–2.5 m) interacting with fine- to medium-grained sand. These types of beaches are characterized by a surf zone with one or two bars up to 100 m wide. The bar is typically traversed by regularly spaced shore-perpendicular rip channels and currents.

Dissipative beaches are produced by high waves (H > 2.5 m) interacting with fine-grained sand. These morphotypes are characterized by gently seaward-sloping beachfaces with low-gradient swash (~1°) and 300–500 m wide surf zone that contains at least two bars. Waves sequentially break on the outer bar first and then on inner bars and in the process dissipate their energy as they move through the surf zone.

Tide-modified beaches are characterized by a RTR that lies between 3 and 10, which implies that the tidal range is increasing and/or wave height is decreasing. This morphodynamic beach type usually has a steeply sloping, cusped, and reflective beachface that is developed in coarser-grained sediments to produce a so-called high-tide beach. Tide-modified morphotypes are fronted by a wide, finer-grained, low-gradient, often featureless, intertidal zone (up to 200 m wide), seaward of which lies a low-tide surf zone that may contain bars and rip channels.

Tide-dominated beaches are produced when the RTR lies between 10 and approximately 50, implying high tides and/or very low waves (H << 0.3 m). These morphotypes are characterized by a low elevation, coarse-grained sediments, irregular, high-tide beach that is fronted by low-gradient (<<1°) intertidal sand or mud flats that may be hundreds of meters wide. Beyond an RTR of 50, tidal flats typically prevail.

An additional morphodynamic beach type is associated with a high-tide reflective beachface that is fronted by intertidal rock flats in middle latitudes. In tropical zones, the high-tide beach may be fronted by a fringing coral reef flat. High latitude morphotypes are seasonally exposed to freezing air and water temperatures that lead to the development of sea ice, shoreface ice, and a frozen snow-covered beach (Short and Woodroffe, 2009).

Summary

Although seemingly simple in appearance, beaches are complex systems where many aspects of their formation are incompletely understood. The morphological results of interactions between processes and materials are categorized in a range of processes-based beach types that are easily recognizable on beaches of the world. Beach processes are observed to operate over myriametric (macro-, meso-, micro-) scales and a range of time frames with grains on the beachface changing by the second to some sand bars that may persist for hundreds of years. Complete understanding of how beaches evolve (accrete) and devolve (erode) over time in different kinds of sedimentary environments provides scope for future

studies that involve observation by various means in the field and laboratory.

Bibliography

Anthony, E. J., and Dolique, F., 2004. The influence of Amazon-derived mud banks on the morphology of sandy, headland-bound beaches in Cayenne, French Guiana: a short- to long-term perspective. *Marine Geology*, **208**, 249–264.

Anthony, E. J., Dolique, F., Gardel, A., and Marin, D., 2011. Contrasting sand beach morphodynamics in a mud-dominated setting: Cayenne, French Guiana. *Journal of Coastal Research*, SI 64 (*Proceedings of the 11th International Coastal Symposium*), pp. 30–34.

Bagnold, R. A., 1941. *The Physics of Blown Sand and Desert Dunes*. New York: Chapman and Hall, 265 p.

Bascom, W. H., 1954. Characteristics of natural beaches. In *Proceedings 4th Conference of Coastal Engineering*. Chicago: Illinois, pp. 163–180.

Bascom, W. H., 1980. *Waves and Beaches*. New York: Doubleday.

Carter, R. W. G., 1988. *Coastal Environments*. San Diego, CA: Academic.

Davidson-Arnott, R. A., 2005. Beach and nearshore instrumentation. In Schwartz, M. L. (ed.), *Encyclopedia of Coastal Science*. Dordrecht: Springer, pp. 130–138.

Davidson-Arnott, R. A., 2009. *Introduction to Coastal Processes and Geomorphology*. Cambridge, UK: Cambridge University Press.

Davidson-Arnott, R. A., and Law, M. N., 1996. Measurement and prediction of long-term sediment supply to coastal foredunes. *Journal of Coastal Research*, **12**(3), 654–663.

Davis, R. A., 1985. Beach and nearshore zone. In Davis, R. A. (ed.), *Coastal Sedimentary Environments*. New York: Springer, pp. 379–444.

Davis, R. A., and FitzGerald, D. M., 2004. *Beaches and Coasts*. Oxford: Blackwell, 419 p.

Dean, R. G., and Dalrymple, R. A., 2002. *Coastal Processes with Engineering Applications*. Cambridge: Cambridge University Press, p. 475.

Dingler, J. R., 2005. Beach processes. In Schwartz, M. L. (ed.), *Encyclopedia of Coastal Science*. Dordrecht, The Netherlands: Springer, pp. 161–168.

Duncan, J. R., 1964. The effects of water table and tide cycle on swash-backwash sediment distribution on beach profile development. *Marine Geology*, **2**, 186–197.

Greenwood, B., 2005. Bars. In Schwartz, M. L. (ed.), *Encyclopedia of Coastal Science*. Dordrecht, The Netherlands: Springer, pp. 120–129.

Guza, R., and Inman, D., 1975. Edge waves and beach cusps. *Journal of Geophysical Research*, **80**(21), 2997–3012.

Hallermeier, R. J., 1981. A profile zonation for seasonal sand beaches from wave climate. *Coastal Engineering*, **4**, 253–277.

Hardisty, J., 1990. *Beaches: Form and Processes*. London: Unwin Hyman, 324 p.

Higgins, C. G., 1984. Piping and sapping: development of landforms by groundwater outflow. In Lafleur, R. G. (ed.), *Groundwater as a Geomorphic Agent*. Boston: Allen and Unwin, pp. 18–58.

Klein, A. H., Filho, L. B., and Schumacher, D. H., 2002. Short-term beach rotation processes in distinct headland bay beach systems. *Journal of Coastal Research*, **18**, 442–458.

Komar, P. D., 1997. *Beach Processes and Sedimentation*. Upper Saddle River, NJ: Prentice Hall, 544 p.

Leatherman, S. P., 2013. Rip currents. In Finkl, C. W. (ed.), *Coastal Hazards*. Dordrecht, The Netherlands: Springer, pp. 811–831.

Otvos, E. G., 1964. Observations on rhomboid beach marks. *Journal of Sedimentary Petrology*, **34**, 683–687.

Otvos, E. G., 1965. Type of rhomboid beach surface patterns. *American Journal of Science*, **263**, 271–276.

Otvos, E. G., 1999. Rain-induced beach processes; landforms from ground water sapping and surface runoff. *Journal of Coastal Research*, **15**(4), 1040–1054.

Pethick, J., 1984. *An Introduction to Coastal Geomorphology*. London: Edward Arnold.

Pilkey, O. H., Neal, W. J., Kelley, J. T., and Cooper, A. G., 2011. *The World's Beaches*. Berkeley, CA: University of California Press, 283 p.

Reussink, B. G., 1998. *Infragravity waves in a dissipative multiple bar system*. Doctoral dissertation, Utrecht, The Netherlands: University of Utrecht, 243 p.

Roelvink, J. A., and Broker, I., 1993. Cross-shore profile models. *Coastal Engineering*, **21**, 163–191.

Shepard, F. P., 1950. *Beach Cycles in S. California*. U.S. Army Corps of Engineers BEB Technical Memo 20, 26 p.

Short, A. D. (ed.), 1999. *Handbook of Beach and Shoreface Morphodynamics*. Chichester, UK: Wiley.

Short, A. D., 2006. Australian beach systems – nature and distribution. *Journal of Coastal Research*, **22**, 11–27.

Short, A. D., 2012. Coastal processes and beaches. *Nature Education Knowledge*, **3**(10), 15.

Short, A. D., and Trembanis, A. C., 2004. Decadal scale patterns in beach oscillation and rotation Narrabeen Beach, Australia – time series, PCA and wavelet analysis. *Journal of Coastal Research*, **20**, 523–532.

Short, A. D., and Woodroffe, C. D., 2009. *The Coast of Australia*. Melbourne: Cambridge University Press.

Sonu, C. J., and van Beek, J. L., 1971. Systematic beach changes in the outer banks. N. Carolina. *Journal of Geology*, **79**, 416–425.

Tamura, T., Horaguchi, K., Saito, Y., Nguyen, V. L., Tateishi, M., Ta, T. K. O., Nanayama, F., and Watanabe, K., 2010. Monsoon-influenced variations in morphology and sediment of a mesotidal beach on the Mekong River delta coast. *Geomorphology*, **116**, 11–23.

Thornton, E. B., Humiston, R. T., and Birkemeier, W., 1996. Bar-trough generation on a natural beach. *Journal of Geophysical Research*, **101**, 12097–12110.

Woodroffe, C. D., 2002. *Coasts — Form and Processes*. Cambridge, UK: Cambridge University Press.

Wright, L. D., and Short, A. D., 1984. Morphodynamic variability of surf zones and beaches: a synthesis. *Marine Geology*, **56**, 93–118.

Wright, L. D., Chappell, J., Thom, B., Bradshaw, M., and Cowell, O., 1979. Morphodynamics of reflective and dissipative beach and inshore systems. South Australia. *Marine Geology*, **32**, 105–140.

Wright, L. D., Guza, R. T., and Short, A. D., 1982. Dynamics of a - high-energy dissipative surf-zone. *Marine Geology*, **45**, 41–62.

Zhang, D. P., 1994. Wave flume experiments on the formation of longshore bars produced by breaking waves. *Science Report, Institute Geoscience, University of Tsukuba*, **15**, 47–105.

Cross-references

Beach
Bed Forms
Coastal Engineering
Coasts
Currents
Dunes
Engineered Coasts
Laminated Sediments
Placer Deposits
Sea Walls/Revetments
Sediment Transport Models
Waves

BED FORMS

Miwa Yokokawa
Laboratory of Geoenvironment, Faculty of Information Science and Technology, Osaka Institute of Technology, Osaka, Japan

The term "bedforms" is used for to describe rhythmic topographic features on the surface of granular beds. A wide variety of such features form in response to specific ranges of hydraulic conditions and grain size. Apart from their intrinsic scientific interest, bedforms are important in both geology and engineering. Large subaqueous bedforms can be obstacles to navigation, and their migration can be a threat to submarine structures. Bedforms also play an important role in determining the resistance to flow. Bedforms are also one of the most useful tools available for interpreting ancient sedimentary environments from outcrops.

When unidirectional flow operates on relatively fine-grained sand (less than 0.7 mm), the following bedforms appear in order as flow "strength" is increased: current ripples, dunes, upper-regime plane bed (absence of bedforms), antidunes, and cyclic steps. If the bed material is coarser than 0.7 mm, the ripple regime is replaced by lower-regime plane bed.

Under purely oscillatory flows over fine-grained sediments, small symmetrical regular straight-crested (2D) ripples, less regular 3D ripples, and large 3D ripples appear with increasing oscillatory velocity magnitude. In the case of long-period oscillatory flows, large dome-like mounds with gentle slopes appear; these are known as "hummocky beds." In the case of coarser sediment, ripples tend to stay straight-crested. When the velocity magnitude becomes large, ripples are washed out to plane bed.

When unidirectional flow is superimposed on oscillatory flow, i.e., combined wave-current flow, bedforms change corresponding to the sum of unidirectional flow velocity and oscillatory flow velocity magnitude. When the unidirectional flow velocity is smaller than a threshold, bedforms are the same as those under purely oscillatory flow. When unidirectional flow velocity increases beyond this threshold, bedforms show characteristic rounded crests and asymmetrical profiles. The threshold at which unidirectional flow affects bedform shape decreases with increasing oscillatory period. When the unidirectional component dominates, large, asymmetric dune-like bedforms appear. On the other hand, when the oscillatory component dominates, hummocky beds appear. These bedforms wash out to plane bed at sufficiently high velocities.

Various bed phase diagrams have been proposed to categorize the relationship between bedforms and hydraulic conditions. In order to construct such diagrams, the relevant parameters which govern the relationships must be specified. In general, bed state is a function of seven parameters. Five parameters are common to all cases: grain size, sediment density, fluid density, fluid viscosity, and sediment submerged specific weight. For unidirectional flow, two more parameters, such as flow velocity and flow depth, are needed. For oscillatory flow, two of the following three parameters must be specified: oscillation period, orbital diameter, and maximum orbital velocity. Dimensional analysis allows the seven variables to be grouped into four dimensionless variables. A large body of experimental research on bedforms under unidirectional flows and short-period oscillatory flows is available. Our knowledge of long-period oscillatory flows and multidirectional combinations of combined waves and currents, however, remains limited.

Bibliography

Bridge, J., and Demicco, R., 2008. *Earth Surface Processes Landforms and Sediment Deposits*. Cambridge, UK/New York: Cambridge University Press, pp. 121–254. Chap. 5, 6, 7.

Garcia, M. H., 2008. Chapter 2 Sediment transport and morphodynamics. In: Garcia, M. H. (ed.), *Sedimentation Engineering.* ASCE (American Society of Civil Engineers), pp. 21–163.

Leeder, M., 2011. Chapter 7 Bedforms and sedimentary structures in flows and under waves. In Leeder, M. (ed.), *Sedimentology and Sedimentary Basins*, 2nd edn. Willey-Blackwell, pp. 132–170.

Southard, J.B., Chapter 12 Bed configurations. In Southard, J. B., 12.090 Introduction to Fluid Motions, Sediment Transport, and Current-Generated Sedimentary Structures, Fall 2006. (MIT OpenCourseWare: Massachusetts Institute of Technology), http://ocw.mit.edu/courses/earth-atmospheric-and-planetary-sciences/12-090-introduction-to-fluid-motions-sediment-transport-and-current-generated-sedimentary-structures-fall-2006, 350-443.

BIOCHRONOLOGY, BIOSTRATIGRAPHY

Felix M. Gradstein
Museum of Natural History, University of Oslo, Oslo, Norway

Biochronology attempts to organize the fossil record in linear time, using the notion that fossil events and fossil zones are organized according to the irreversible process of evolution.

The key to biochronology and its building blocks is fossil events. A fossil or paleontological event is the presence of a fossil taxon in its time context, derived from its position in a rock sequence. Most commonly used are first appearance and last appearance datums (FAD and LAD). Since the first or last appearance datum may be difficult to recognize or distinguish where specimen numbers dwindle or get obscured by "noise" (like reworking of fossil tests very common with the tiny nannofossils), it can be advantageous to substitute with first and last consistent (or common) appearances. A first or last appearance datum is called consistent when such stratigraphic range

end points are part of an observed continuous stratigraphic range.

If the fossil record encountered in stratigraphic sections that we want to correlate and calibrate in time would be ubiquitous and perfect, i.e., if only time would control the appearance, range, and disappearance of taxa, then biostratigraphy would be a straightforward exercise. The science of biochronology, as developed for the evolutionary first and last occurrence datums of ocean plankton, would be a matter of systematic bookkeeping on a worldwide scale, only constrained by taxonomic deliberations. Unfortunately, the paleontological record is highly imperfect.

Uncertainty factors may be summarized as follows:

1. Quality and quantity of sampling
2. Specimen frequency of fossil taxa
3. Confidence of taxonomic identification
4. Influence of environmental change on the stratigraphic range of taxa
5. Differential rate of taxon evolution in different parts of the world
6. Time lag in migration of taxa, where correlation is over large distances or across major environmental barriers

Hence, biochronology almost always requires careful calibration with independent geomagnetic reversals and stable isotope correlation frameworks.

Biochronology is reaching a pinnacle in the massive fossil event datasets generated with TimeScale Creator software (http://www.tscreator.org). The method and data system confidently link all events in the evolutionary "organic continuum" in an elegant linear time framework, calibrated to Geologic Time Scale 2012 (see Geologic Time Scale). A recent calibration of Cretaceous and Cenozoic planktonic foraminifera and calcareous nannofossils of the temperate to tropical marine realm is by Anthonissen and Ogg (2012). Syntheses for siliceous, organic, and other microfossil biostratigraphy are summarized in the appropriate chapters in *The Geologic Time Scale* (Gradstein et al., 2012), and detailed and updated versions of all stratigraphic scales can be accessed as datasets and graphics at the TimeScale Creator website.

Special mention is made of the detailed and high-resolution (deep time) conodont-foraminifera-ammonoid composite zonation for the Carboniferous, with over 35–40 zones constrained by 36 radiometric dates employed in timescale building for this period (Davydov et al., 2012). Particularly in younger parts of the Carboniferous zonal event, resolution is resolved at a biochronologic scale that provides insight in biota migrations due to the waxing and waning of massive Gondwana supercontinent glaciations.

Summary

Biochronology attempts to order and scale fossil events and fossil ranges in linear time.

Bibliography

Anthonissen, D. E., and Ogg, J. G., 2012. Cenozoic and cretaceous biochronology of planktonic foraminifera and calcareous nannofossils. In Gradstein, F. M. (ed.), *The Geologic Time Scale 2012*. Amsterdam: Elsevier, pp. 1083–1128.

Davydov, et al., 2012. for reference see The Geologic Time Scale.

Gradstein, F. M., et al., 2012. *The Geologic Time Scale*. Amsterdam: Elsevier.

BIOGENIC BARIUM

Graham Shimmield
Bigelow Laboratory for Ocean Sciences, East Boothbay, ME, USA

Biogenic barium usually occurs as discrete microcrystals of the refractory mineral, barite ($BaSO_4$). It may be found in the water column (in the tests of both live and dead planktonic species), in benthic foraminifera, in coral skeletons, and in the underlying sediment. The earliest observations of enriched barium (usually identified as barium concentrations exceeding typical shale or sediment concentrations), and attributed to biological processes, are the work of Revelle et al. (1955) working in the equatorial divergence of the Pacific Ocean. Dehairs et al. (1980) and Bishop (1988) showed that barite ($BaSO_4$) was precipitated in decaying suspended marine particulate matter (particularly diatoms) in oceanic waters. Some studies have suggested that biogenic barium may occur in heavy mineral granules functioning as statoliths in statocyst organs and within protozoans such as Xenophyophoria and Loxodes. Biogenic barium distribution and concentration have been studied in benthic foraminifera and corals as a tracer of bottom water nutrients and upwelling, respectively.

Biogenic barium in sediments is often found in water underlying areas of high productivity. Bishop (1988) has studied the barium content of large and small particles in the Gulf Stream, and Schmitz (1987) has illustrated the use of Ba as a tracer of Indian Ocean plate movement beneath the equatorial upwelling zone on a timescale of millions of years. Virtually, all ocean basins display enrichment of biogenic barium where productivity is elevated and with time (paleoproductivity). Shimmield (1992) suggested that barite-secreting organisms may be confined to a rather discrete zone within the coastal upwelling productivity belt, seaward of the shelf break (under a different nutrient regime), and as a consequence shallow-water, organic-rich sediments may receive little biogenic barium, or the sedimentary barite undergoes diagenesis during sulfate reduction (see below). A similar distribution of biogenic barium was noted by Calvert and Price (1983) in their work off Namibia.

The refractory nature of barite was remarked on in the earliest work by Dymond (1981), something he called a

"dissolution residue." The association of biogenic Ba, opal, and biogenic sedimentation has been described by many authors (see reviews in Schmitz, 1987; Gingele et al., 1999). These observations have opened the potential to use biogenic barium downcore distributions as an important proxy for paleoproductivity, given that both organic carbon and opal may suffer from remineralization and dissolution. An important step in quantifying past productivity is to establish the relationship between biogenic barium and organic carbon in sediment traps (Dymond et al., 1992; Francois et al., 1995). Using algorithms developed from empirical observations, downcore variations in biogenic barium flux have been converted to paleoprimary production. This approach has a number of assumptions and potential drawbacks. In particular, it is necessary to calculate the biogenic component of the total barium content in the sediment. This is usually achieved by normalization to lithogenic metals such as aluminum or titanium. There may be additional sources of barium to the sediment from hydrothermal systems or benthic organisms such as xenophyophores. Finally, although barite is very refractory under oxic conditions, during sulfate reduction in anaerobic sediments, barite dissolution may occur.

Bibliography

Bishop, J. K. B., 1988. The barite-opal-organic-carbon association in oceanic particulate matter. *Nature*, **332**, 341–343.

Calvert, S. E., and Price, N. B., 1983. Geochemistry of Namibian shelf sediments. In Suess, E., and Thiede, J. (eds.), *Coastal Upwelling, Part A*. New York: Plenum, pp. 337–375.

Dehairs, F., Chesselet, R., and Jedwab, J., 1980. Discrete suspended particles of barite and the barium cycle in the open ocean. *Earth and Planetary Science Letters*, **49**, 528–550.

Dymond, J., 1981. Geochemistry of Nazca plate surface sediments: an evaluation of hydrothermal, biogenic, detrital, and hydrogenous sources. *Memoirs of the Geological Society of America*, **154**, 133–173.

Dymond, J., Suess, E., and Lyle, M., 1992. Barium in deep-sea sediment: a geochemical proxy for paleoproductivity. *Paleoceanography*, **7**(2), 163–181.

Francois, R., Honjo, S., Manganini, S. J., and Ravizza, G. E., 1995. Biogenic barium fluxes to the deep-sea: implications for paleoproductivity reconstruction. *Global Biogeochemical Cycles*, **9**, 289–303.

Gingele, F. X., Zabel, M., Kasten, S., Bonn, W. J., and Nurnberg, C. C., 1999. Biogenic barium as a proxy for paleoproductivity: methods and limitations of application. In Fischer, G., and Wefer, G. (eds.), *Use of Proxies in Paleoceanography*. Berlin: Springer, pp. 345–364.

Revelle, R., Bramelette, M., Arrenhius, G., and Goldberg, E. D., 1955. Pelagic sediments of the Pacific. *Geological Society of America, Special Paper*, **62**, 221–235.

Schmitz, B., 1987. Barium, high productivity, and northward wandering of the Indian continent. *Paleoceanography*, **2**, 63–77.

Shimmield, G. B., 1992. Can sediment geochemistry record changes in coastal upwelling paleoproductivity? Evidence from northwest Africa and the Arabian Sea. In Summerhayes, C., Prell, W., and Emeis, K. (eds.), *Upwelling Systems Since the Early Miocene*. London: Geological Society. Geology Society Special Publication, Vol. 63, pp. 29–46.

BIOTURBATION

Gerhard Graf
Institute for Biological Sciences, University of Rostock, Rostock, Germany

Definition

Bioturbation is the mixing and displacement of particles in marine and freshwater sediments caused by benthic fauna mainly during foraging and the construction of burrows. As a result particulate proxies and microfossils such as tests of foraminifera deposited at the seafloor may not be found in the time slice corresponding to its deposition, and the interpretation of the geological record can be hampered. Other effects of animal activity, such as biodeposition and bioresuspension, but also fluid transport will not be considered in this section although they are essential for biogeochemical cycles and are used as subprocesses of bioturbation in recent biological literature (cf. Kristensen et al. 2012).

Measurement and modeling

In geological sciences, mainly natural radioactive tracers like ^{210}Pb, ^{234}Th, or ^{7}Be but also chlorophyll a or stained sand grains have been used for a quantitative description. A basic equation for sediment mixing was provided by Berner (1980).

$$\frac{\partial C}{\partial t} = \frac{\partial}{\partial x}\left(D_b(x)\frac{\partial C}{\partial x}\right) - \omega\frac{\partial C}{\partial x} \pm R(C,x,t)$$

C = concentration of tracer, t = time, x = depth, D_b = mixing coefficient, ω = burial velocity, R = reaction term for the tracer

It describes particle mixing in analogy to molecular diffusion. This assumption holds true in the case of many animals moving particles in a stochastic way in small steps (local mixing). Statistically this creates a transport of tracers along the concentration gradient, as does the Brownian movement on the molecular level, and can be calculated via Fick's law of diffusion. The mixing coefficient D_b provides a quantitative measure.

Some animals transport food particle directly in one step from the surface to depth, or particles may drop into open burrows. In these cases the diffusion analogy is inadequate, and this advective transport (nonlocal mixing) has to be considered separately, i.e., the step length and frequency of such events have to be determined and to be included into the model, as, for example, in the gallery-diffusion model by Francois et al. (2002).

Order of magnitude

From published data, Boudreau (1994) calculated a worldwide mean mixing depth of 9.8 ± 4.5 cm. It is, however, well documented that animal burrows may reach as deep as 2 m (Thalassinidea). Mixing coefficients D_b may range from 0.0002 to 370 cm^2 years^{-1}. The latter results are

highly dependent on the habitat and the tracers used. The shorter the half-life of the tracer, the higher is D_B. This result is mainly explained by the fact that some animals are highly selective and prefer fresh organic matter.

So far attempts to find general relationships between sediment mixing and biomass or organic carbon content failed, indicating the strong species-specific effect of bioturbation.

Bibliography

Berner, R. A., 1980. *Early Diagenesis: A Mathematical Approach*. Princton: Princton University Press.

Boudreau, B. P., 1994. Is burial velocity a master parameter for bioturbation? *Geochimica et Cosmochimica Acta*, **58**, 1243–1249.

Francois, F., Gerino, M., Stora, G., Durbec, J.-P., and Poggiale, J.-C., 2002. Functional approach to sediment reworking by gallery-forming macrobenthic organisms: modeling and application with the polychaete Nereis diversicolor. *Marine Ecology Progress Series*, **229**, 127–136.

Kristensen, E., Penha-Lopes, G., Delefosse, M., Valdemarsen, T., Quintana, C. O., and Banta, G. T., 2012. What is bioturbation? The need for a precise definition for fauna in aquatic sciences. *Marine Ecology Progress Series*, **446**, 285–302.

BLACK AND WHITE SMOKERS

Margaret K. Tivey
Marine Chemistry & Geochemistry, Woods Hole Oceanographic Institution, Woods Hole, MA, USA

Synonyms

Active vent deposit; Black chimney, White chimney; Black smoker chimney, White smoker chimney; Hydrothermal chimney

Definition

Black and white smokers. Chimney-like edifices composed of mixtures of copper-, iron-, and zinc-sulfide minerals and calcium- and barium-sulfate minerals. They form as very hot (up to ~400 °C or 750 °F) fluids exit very young seafloor and mix with cold seawater, with the high-temperature fluids passing through channels within the edifices into the deep ocean.

Introduction

Black and white smokers are the portions of seafloor hydrothermal vent deposits through which ~200 °C–400 °C hydrothermal fluids travel and exit into the deep ocean, <1,000–5,000 m below sea-level. The hot fluids form as cold seawater percolates down into young, still hot seafloor near the spreading axes of the mid-ocean ridges and spreading centers in back-arc basins; during its transit, the seawater exchanges heat and undergoes chemical reactions with the young oceanic crust. The seawater loses oxygen and sulfate, becomes more acidic (pH decreases), and becomes enriched in metals (e.g., Fe, Mn, Cu, Zn, Pb) and hydrogen sulfide, and its temperature increases from ~2 °C to >400 °C (German and Von Damm, 2006). The hot fluid is very buoyant (because its density decreases to approximately two-thirds of the original density as it is heated to >400 °C) and rises rapidly to the seafloor, exiting at meter-per-second flow rates (Bischoff and Rosenbauer, 1985; Spiess et al., 1980; see "Hydrothermal Vent Fluids (Seafloor)"). When the hot, metal- and sulfide-rich, oxygen-poor fluid exits and mixes with cold, sulfate-rich, metal-poor seawater, minerals precipitate rapidly as chimney-like edifices and as particles within plumes (with a smokelike appearance) above the edifice – see Figure 1.

Discovery

Venting of hydrothermal fluids from the youngest portions of the seafloor along the mid-ocean ridges was first observed in 1977 along the Galapagos Rift where unusual biological communities were found associated with warm vent fluids (17 °C, much warmer than the surrounding 2 °C seawater); the presence of these warm fluids had been predicted based on measurements of heat flow (see "Marine Heat Flow") and bottom seawater thermal anomalies close to the mid-ocean ridge (Corliss et al., 1979). In 1978, massive sulfide deposits that likely formed from much higher temperature fluids were found near 21°N latitude on the East Pacific Rise about 650 m west of the spreading axis (Francheteau et al., 1979). The first actively venting black and white smokers were subsequently discovered in 1979, along the spreading axis of the East Pacific Rise (Spiess et al., 1980) not far from where the deposits were found a year earlier.

The hot fluids were observed exiting "stacks" or "chimneys" that were 1–5 m tall, composed of copper-, iron-, and zinc-sulfide minerals and the mineral anhydrite (calcium sulfate) (Spiess et al., 1980). The observed black chimneys, or black smokers, resembled organ pipes ≤30 cm in diameter and emitted hot (>350 °C) fluid with dark-colored (black) precipitates suspended within the exiting fluid (Spiess et al., 1980). The white chimneys, or white smokers, were covered with worm tubes (making them light-colored) and emitted cooler (<330 °C) fluids at slower flow rates with light-colored precipitates suspended within exiting waters (Spiess et al., 1980; Haymon and Kastner, 1981).

Formation of black smoker chimneys

Black smoker chimneys form in two stages (Haymon, 1983; Goldfarb et al., 1983): (1) deposition of an anhydrite ($CaSO_4$)-dominated wall as hot, calcium-rich vent fluid mixes turbulently with cold, sulfate- and calcium-rich seawater, followed by (2) deposition of a layer of sulfide minerals against the inner side of the anhydrite layer as the Stage 1 anhydrite wall prevents rapid mixing between the hot fluid flowing inside the chimney and the cold

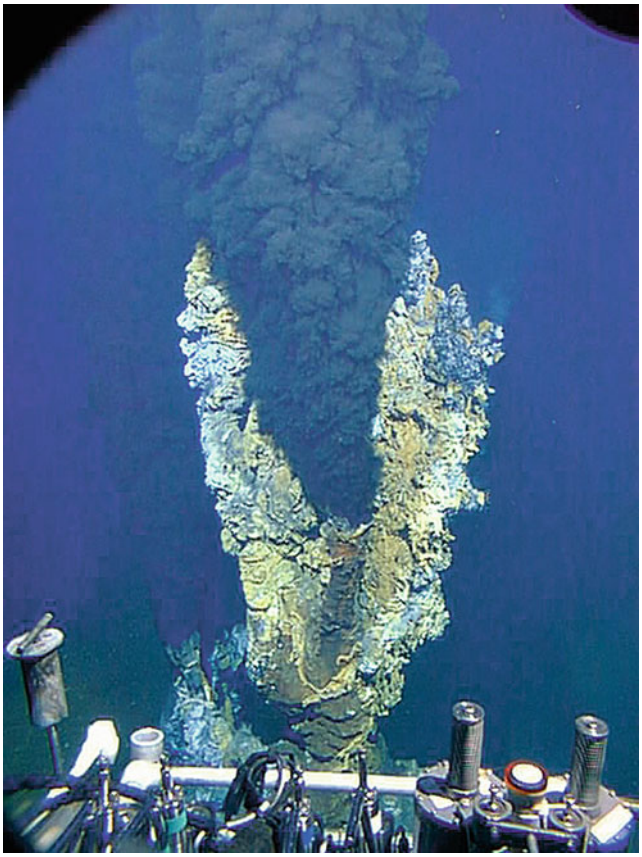

Black and White Smokers, Figure 1 Hot (347 °C) vent fluid exits multiple black smokers on the chimney edifice "Homer" near 17.5°S latitude on the southern East Pacific Rise (Courtesy Woods Hole Oceanographic Institution; M. Lilley and K. Von Damm chief scientists).

seawater present on the outside of the chimney. Chalcopyrite ($CuFeS_2$) is dominant if temperature is >330 °C and pyrite (FeS_2) and wurtzite ((Zn, Fe)S) occur at lower temperatures. Infiltration of seawater and hydrothermal fluid components across the porous wall also results in the deposition of sulfide and sulfate minerals and silica in the interstices of the wall, which gradually makes the chimney less porous and more metal-rich – see Figure 2. Interaction of fluids and biota on chimney exteriors can also result in the formation of an iron-sulfide-rich outermost layer on the chimney (Juniper et al., 1992).

Rapid formation of the Stage 1 chimney wall (it can form at rates up to 30 cm per day; Goldfarb et al., 1983) is in part a consequence of anhydrite being an unusual mineral that is more soluble at low temperatures than at high temperatures; if seawater is heated to ~150 °C or greater, anhydrite precipitates (Bischoff and Seyfried, 1978). When the very hot vent fluid exits at meter-per-second velocities into seawater, mixtures above ~150 °C will be saturated in anhydrite, with the sulfate coming from seawater and the calcium from both the vent fluid and seawater (Styrt et al., 1981; Albarède et al., 1981). Metal sulfides and oxides (zinc sulfide, iron sulfide, copper-iron sulfide, manganese oxide, and iron oxide) also precipitate from the vent fluid and vent fluid/seawater mixtures as fine-grained particles. Some of these particles become trapped within and between grains of anhydrite within the Stage 1 chimney walls, giving the anhydrite, which is clear to white in its pure form, a gray to black color (Goldfarb et al., 1983; Haymon, 1983). The remaining particles form a plume of "smoke" above the chimney. Because bottom seawater is denser than the mix of seawater and hydrothermal fluid in the plume, the plume rises a few 100 m above the seafloor to a depth where it is of the same buoyancy as the surrounding ocean water (see "Hydrothermal Plumes").

Once the initial anhydrite-dominated framework is in place, chalcopyrite (or chalcopyrite and pyrite or chalcopyrite and wurtzite for lower temperature black smokers) precipitates on the inner surface of the chimney. Observed young chimney walls are thin, less than a centimeter to a few centimeters, with one side of the wall very hot and one side much colder. The porous chimney wall is subject to steep gradients of temperature and concentrations of elements. As the chimney evolves, the innermost layer thickens (recovery of a chimney known to be only 1 year old had an innermost chalcopyrite layer that was ~1 cm thick; Koski et al., 1994). At the same time that the innermost layer is thickening, aqueous ions, including copper, iron, hydrogen, oxygen, sulfide, sulfate, zinc, sodium, chloride, and magnesium, are transported from areas of high to low concentrations (by diffusion). These elements also are carried by fluids flowing across the wall from areas of high to low pressure (by advection). As a result of these processes, minerals become saturated and precipitate in the pore spaces within the chimney walls, and favorable conditions for microorganisms are established in the outer parts of the chimney walls. In particular, within the chimney walls at temperatures less than ~120 °C, the steep temperature and concentration gradients provide combinations of reducing chemicals from vent fluids (hydrogen, hydrogen sulfide, ferrous iron) and oxidizing chemicals from seawater (oxygen, sulfate, ferric iron) that can be used by microorganisms (bacteria and archaea) as sources of energy (see "Chemosynthetic Life"; Jannasch, 1995). Larger organisms (e.g., alvinellids and paralvinellids; Haymon and Kastner, 1981; Juniper et al., 1992) also reside on the exteriors of chimneys, and their tubes can become incorporated into chimney walls – see Figure 3. As the chimney grows, earlier-formed minerals, as they are exposed to hotter fluids, can be replaced by later-formed minerals.

Formation of white smoker chimneys

The style of mixing between vent fluid and seawater differs in chimneys that emit lower-temperature, white to clear fluids (~200–330 °C). One major reason for this is that the vent fluid is flowing more slowly. Because the

Black and White Smokers, Figure 2 Schematic drawing showing Stage 1 and Stage 2 growth of black smoker chimneys (After Haymon, 1983 and Goldfarb et al., 1983; figure from Tivey, 1998, courtesy Woods Hole Oceanographic Institution).

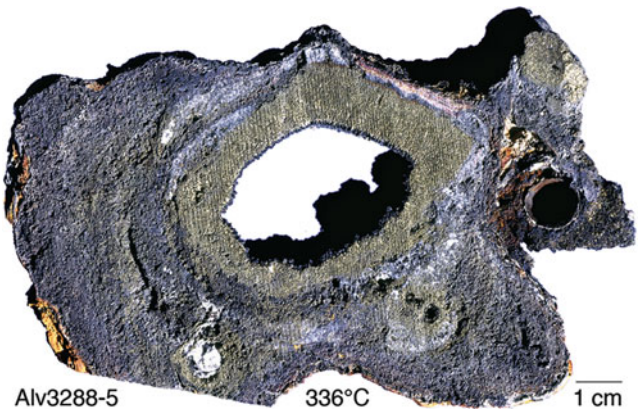

Black and White Smokers, Figure 3 Photograph of a slab taken perpendicular to the open channel across a black smoker chimney that was venting 336 °C fluid, from the southern East Pacific Rise near 21.5°S. The innermost layer (~1 cm thick) is composed of chalcopyrite (*gold* in color), and the outer 0.5–3 cm layer is composed of a mixture of anhydrite and sulfide minerals (*gray* in color). The fossilized tube of an alvinellid is embedded in the chimney wall (*right* side of image) (courtesy Woods Hole Oceanographic Institution).

fluid percolates less vigorously through the porous spires, a greater percentage of metal from the fluid precipitates within the deposit instead of being lost to the ocean within particle-laden plumes (e.g., Haymon and Kastner, 1981; Koski et al., 1994). Some of the white smoker chimneys are dominated by zinc- and iron-sulfide minerals, which form both an initial framework and infilling material (Koski et al., 1994 – see Figure 4). Others contain abundant barite and silica, both as initial framework material and as infilling material, with barite then co-precipitating with silica and sulfide minerals (Hannington and Scott, 1988). Many white smokers lack anhydrite, consistent with a lack of entrained seawater as they form. In contrast to black smokers, where flow is rapid through open conduits of >1 cm diameter, flow in white smokers is through narrow, anastomosing conduits that seal over time, commonly diverting flow horizontally (Fouquet et al., 1993; Koski et al., 1994). Beehive structures or diffusers are another type of smoker found at some vent fields. They have a bulbous morphology, interior temperatures only slightly less than for black smoker chimneys, highly porous interiors, and high-temperature (relative to black

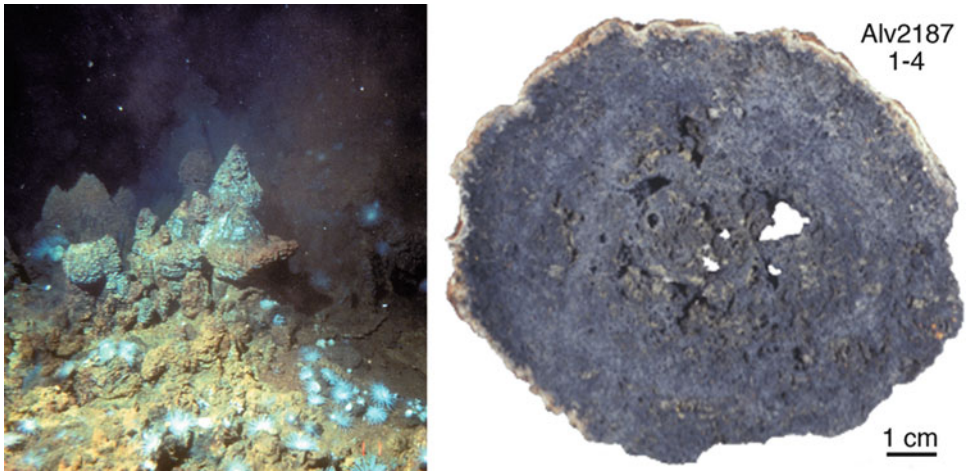

Black and White Smokers, Figure 4 *Left image* is of white smoker chimneys (venting 250–300 °C fluids) from the Kremlin area on the TAG active hydrothermal mound at 26°N on the Mid-Atlantic Ridge (Courtesy of Woods Hole Oceanographic Institution; Peter Rona chief scientist); *right image* is a photograph of a slab taken perpendicular to the axis of one of the Kremlin chimneys, composed dominantly of zinc-sulfide – note the absence of large conduits and prevalence of very narrow channelways (courtesy of Woods Hole Oceanographic Institution).

and white smoker chimneys) exteriors (up to 70 °C; Fouquet et al., 1993; Koski et al., 1994). They form from less focused high-temperature fluids that exhibit slower flow rates than those from black smokers; as in white smoker chimneys, some flow is diverted and occurs through sides of these smokers (Fouquet et al., 1993; Koski et al., 1994). Within some vent fields, hot fluids are trapped beneath overhanging ledges, termed flanges; fluids percolate up through the porous flange layers or flow horizontally and "waterfall" upwards over the lip of the flange (Delaney et al., 1992).

Carbonate-rich chimneys

Very different types of chimneys are found at the Lost City vent field, located 15 km from the axis of the Mid-Atlantic Ridge. The Lost City hydrothermal system is hosted in mantle rocks (peridotite and serpentinite – see "Peridotites"), and the venting fluids have a higher pH than seawater, low metal and sulfide concentrations, and low temperature (<100 °C) relative to black smoker and white smoker fluids (Kelley et al., 2005); the very tall spires being deposited from these fluids are composed of calcium carbonate and magnesium hydroxide minerals (calcite and/or aragonite ($CaCO_3$) and brucite ($MgOH_2$)) that are saturated in the high pH, carbonate- and hydroxide-rich fluids.

Summary and conclusions

The morphologies of actively venting seafloor hydrothermal deposits and the composition and appearance of their hydrothermal plumes reflect the compositions of the fluids (hydrothermal fluid and seawater) from which they form, and the styles of flow and mixing of these fluids. "Black smoker" chimneys with conduit diameters of <2–10 cm form from very high-temperature (>330–400 °C) fluids that flow at rates of meters per second, and the turbulent mixing that results when this fluid exits into seawater results in the formation of particle-laden plumes reminiscent of black smoke. "White smoker" chimneys form from lower-temperature (~200–330 °C) vent fluids that flow less vigorously through anastomosing narrow conduits that can become blocked resulting in diversion of flow; a greater percentage of metals are trapped and deposited within these chimneys than within black smokers, and they tend to be richer in zinc because of the lower temperatures that result in saturation and precipitation of zinc-sulfide minerals.

Over time, collapse and incorporation of these different types of chimneys and flanges onto and into mounds, and subsequent reworking of this material as hot fluids flow through the mounds, forms larger deposits. These larger deposits (see "Volcanogenic Massive Sulfides" and "Marine Mineral Resources") found along the mid-ocean ridges and along the spreading centers within back-arc basins are analogs for some types of ore deposits found on land (e.g., Cyprus-type massive sulfide ore deposits; Francheteau et al., 1979).

Bibliography

Albarède, F., Michard, A., Minster, J.-F., and Michard, G., 1981. $^{87}Sr/^{86}Sr$ ratios in hydrothermal waters and deposits from the East Pacific Rise at 21°N. *Earth and Planetary Science Letters*, **55**, 229–236.

Bischoff, J. L., and Rosenbauer, R. J., 1985. An empirical equation of state for hydrothermal seawater (3.2 percent NaCl). *American Journal of Science*, **285**, 725–763.

Bischoff, J. L., and Seyfried, W. E., Jr., 1978. Hydrothermal chemistry of seawater from 25° to 350°C. *American Journal of Science*, **278**, 838–860.

Corliss, J. B., Dymond, J., Gordon, L. I., Edmond, J. M., von Herzen, R. P., Ballard, R. D., Green, K., Williams, D.,

Bainbridge, A., Crane, K., and van Andel, T. H., 1979. Submarine thermal springs on the Galapagos Rift. *Science*, **203**, 1073–1083.
Delaney, J. R., Robigou, V., McDuff, R. E., and Tivey, M. K., 1992. Geology of a vigorous hydrothermal system on the Endeavour Segment, Juan de Fuca Ridge. *Journal of Geophysical Research*, **97**, 19663–19682.
Fouquet, Y., Wafik, A., Cambon, P., Mevel, C., Meyer, G., and Gente, P., 1993. Tectonic setting, mineralogical and geochemical zonation in the Snake Pit sulfide deposit (Mid-Atlantic Ridge at 23°N). *Economic Geology*, **88**, 2018–2036.
Francheteau, J., Needham, H. D., Choukroune, P., Juteau, T., Seguret, M., Ballard, R. D., Fox, P. J., Normark, W., Carranza, A., Cordoba, D., Guerrero, J., Rangin, C., Bougault, H., Cambon, P., and Hekinian, R., 1979. Massive deep-sea sulphide ore deposits discovered on the East Pacific Rise. *Nature*, **277**, 523–528.
German, C., and Von Damm, K., 2006. Hydrothermal processes. In Holland, H. D., and Turekian, K. K. (eds.), *Treatise on Geochemistry, volume 6: The Oceans and Marine Chemistry*. London: Elsevier, pp. 181–222.
Goldfarb, M. S., Converse, D. R., Holland, H. D., and Edmond, J. M., 1983. The genesis of hot spring deposits on the East Pacific Rise, 21N. In Ohmoto, H., and Skinner, B. J. (eds.), *The Kuroko and Related Volcanogenic Massive Sulfide Deposits*. New Haven, Conn: Economic Geology Publication. Economic Geology Monograph, Vol. 5, pp. 184–197.
Hannington, M. D., and Scott, S. D., 1988. Mineralogy and geochemistry of a hydrothermal silica- sulfide-sulfate spire in the caldera of Axial Seamount, Juan de Fuca Ridge. *Canadian Mineralogist*, **26**, 603–625.
Haymon, R. M., 1983. Growth history of hydrothermal black smoker chimneys. *Nature*, **301**, 695–698.
Haymon, R. M., and Kastner, M., 1981. Hot spring deposits on the East Pacific Rise at 21°N: preliminary description of mineralogy and genesis. *Earth and Planetary Science Letters*, **53**, 363–381.
Jannasch, H., 1995. Microbial interactions with hydrothermal fluids. In Humphris, S. E., Zierenberg, R. A., Mullineaux, L. S., and Thomson, R. E. (eds.), *Seafloor Hydrothermal Systems*. Washington, DC: American Geophysical Union. American Geophysical Union Monograph, Vol. 91, pp. 273–296.
Juniper, S. K., Jonasson, I. R., Tunnicliffe, V., and Southward, A. J., 1992. Influence of a tube-building polychaete on hydrothermal chimney mineralization. *Geology*, **20**, 895–898.
Kelley, D. S., Karson, J. A., Fruh-Green, G. L., Yoerger, D. R., Shank, T. M., Butterfield, D. A., Hayes, J. M., Schrenk, M. O., Olsen, E. J., Proskurowski, G., Jakuba, M., Bradley, A., Larson, B., Ludwig, K., Glickson, D., Buckman, K., Bradley, A. S., Brazelton, W. J., Roe, K., Elend, M. J., Delacour, A., Bernasconi, S. M., Lilley, M. D., Baross, J. A., Summons, R. E., and Sylva, S. P., 2005. A serpentinite-hosted ecosystem: the Lost City hydrothermal field. *Science*, **307**, 1428–1434.
Koski, R. A., Jonasson, I. R., Kadko, D. C., Smith, V. K., and Wong, F. L., 1994. Compositions, growth mechanisms, and temporal relations of hydrothermal sulfide-sulfate-silica chimneys at the northern Cleft segment, Juan de Fuca Ridge. *Journal of Geophysical Research*, **99**, 4813–4832.
Spiess, F. N., Macdonald, K. C., Atwater, T., Ballard, R., Carranza, A., Cordoba, D., Cox, C., Diaz Garcia, V. M., Francheteau, J., Guerrero, J., Hawkins, J., Haymon, R., Hessler, R., Juteau, T., Kastner, M., Larson, R., Luyendyk, B., Macdougall, J. D., Miller, S., Normark, W., Orcutt, J., and Rangin, C., 1980. East pacific rise: hot-springs and geophysical experiments. *Science*, **207**, 1421–1433.
Styrt, M. M., Brackman, A. J., Holland, H. D., Clark, B. C., Pisutha-Arnold, V., Eldridge, C. S., and Ohmoto, H., 1981. The mineralogy and the isotopic composition of sulfur in hydrothermal sulfide/sulfate deposits on the East Pacific Rise, 21°N latitude. *Earth and Planetary Science Letters*, **53**, 382–390.
Tivey, M. K., 1998. How to build a black smoker chimney: the formation of mineral deposits at mid-ocean ridges. *Oceanus*, **41**, 68–74.

Cross-references

Chemosynthetic Life
Hydrothermal Plumes
Hydrothermal Vent Fluids (Seafloor)
Hydrothermalism
Marine Heat Flow
Marine Mineral Resources
Marginal Seas
Oceanic Spreading Centers
Peridotites
Volcanogenic Massive Sulfides

BOTTOM SIMULATING SEISMIC REFLECTORS (BSR)

Jürgen Mienert and Stefan Bünz
Centre for Arctic Gas Hydrate, Environment and Climate (CAGE), UiT The Arctic University of Norway, Tromsø, Norway

Definition

A seismic reflection occurring in the upper few hundred meters of marine sediments mimicking the seafloor, crosscutting sediment layers, and showing a phase reversal is known as a "bottom-simulating reflector." Such a gas hydrate-related BSR originates from a large impedance contrast between a layer of gas-hydrated sediment above and a free gas layer below. A diagenetic-related BSR occurs at the opal-A/opal-CT transition zone, lies often deep and outside the base of the gas hydrate stability zone, shows no phase reversal, and does not always mimic the seafloor.

Introduction

The intent of this article is to describe the two most commonly observed bottom-simulating reflectors (BSRs). The term BSR stems from their principal characteristic that these reflectors mimic the seafloor topography in marine seismic reflection data thereby crosscutting sedimentary strata. BSRs are known to occur in continental margin sediments in regions of gas hydrate and free gas (Shipley et al., 1979) and/or in siliceous ooze (diatoms, radiolaria, silica sponges, silicoflagellates) bearing sedimentary formations (Hein et al., 1978). The largest silica contribution comes from diatoms (Holland and Turekian, 2003), while the largest methane contribution derives from methane-producing Archaea in sub-seafloor sediments (e.g., Kotelnikova, 2002).

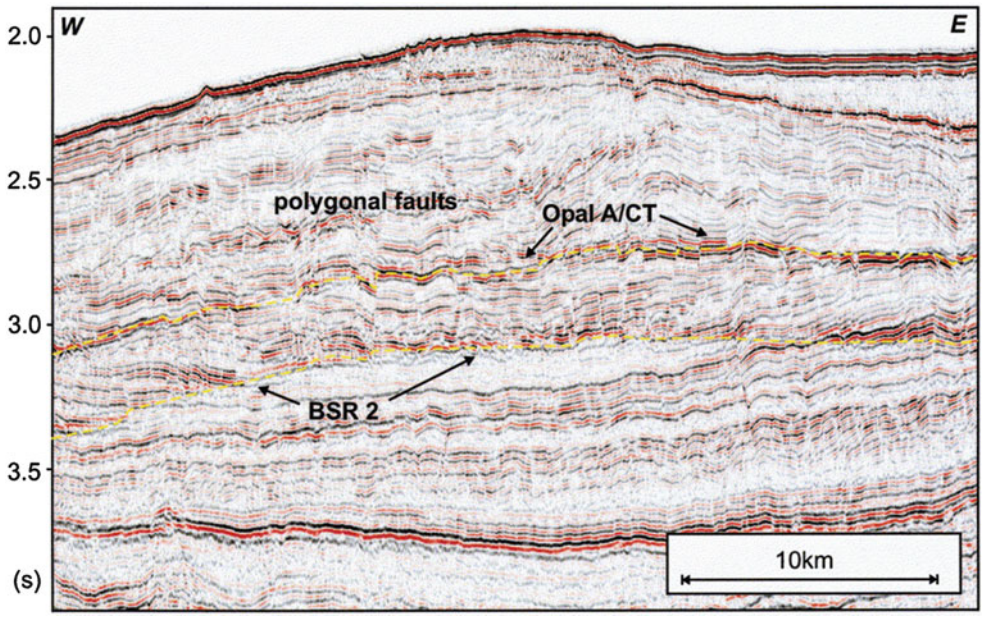

Bottom Simulating Seismic Reflectors (BSR), Figure 1 Reflection seismic profile from the mid-Norwegian margin siliceous sedimentary formation showing an example of an opal-A/opal-CT BSR. The BSR and amplitudes are offset by polygonal faults. The origin of BSR 2 is speculative and may be related to transformation from smectite to illite at higher temperatures (Figure is from Berndt et al., 2004, Figure 4).

Diagenesis-related BSR

Siliceous ooze occurs in a wide range of sedimentary basins indicating times of higher ocean productivity, for example, along equatorial, polar, or coastal upwelling regions (Holland and Turekian, 2003). With increasing burial depth, the temperature and pressure increases, resulting in the dissolution of the siliceous skeletons. The dissolution process causes a collapse of the siliceous framework and a geochemical reaction that converts amorphous opal-A into opal-CT (e.g., Hesse, 1989; Knauth, 1994). Deep-sea drilling project studies allowed documenting the chemical, mineralogical, and structural changes occurring during this process with increasing depth (e.g., Hurd and Birdwhistell, 1983). As a consequence of the skeleton dissolution, an interface develops where the opal-CT formation causes an increase in density and compressional-wave velocity and a decrease in porosity and permeability (e.g., Tribble et al., 1992). If the seismic impedance contrast between opal-A (lower density and velocity and higher porosity and permeability) and opal-CT becomes large enough, a seismic reflector with a positive polarity occurs (Figure 1) (Berndt et al., 2004). It is believed that the temperature increase with burial depth is the main parameter controlling the opal-A/opal-CT transition aside from the time since burial, type of surrounding sediment material, and interstitial waters (e.g., Hein et al., 1978). The opal-A/opal-CT diagenesis causes a volume reduction of as much as 30–40 % (Davies and Cartwright, 2002). Since large areas of siliceous ooze exist in sedimentary formations, a diagenetic BSR (Figure 1) often shows a very large lateral extent, which is uncommon for gas hydrate-/free gas-related BSRs. Moreover, diagenetic BSRs are believed to develop at greater depth below the seafloor, at temperatures (35–50 °C) where hydrate is normally no longer stable (Berndt et al., 2004).

Opal-A/opal-CT BSRs have been reported from many areas containing siliceous sediments such as from the mid-Norwegian margin (e.g., Brekke, 2000; Berndt et al., 2004) (Figure 1). Often, polygonal faults occur in conjunction with diagenetic BSRs as they preferably form in similar types of sediments (Figure 1) (Cartwright and Dewhurst, 1998; Davies and Cartwright, 2002). Polygonal faults show an interruption and vertical offset of continuous reflections leading to short reflection segments. The BSR may be difficult to identify if it runs parallel to the strata, because normally it also does not show a reduced instantaneous frequency (Berndt et al., 2004). The BSR has a strong amplitude, has an apparent polarity that is positive, lies deeper than a gas hydrate-related BSR, and is often interrupted by polygonal faults.

Gas hydrate-related BSR

Gas hydrates occur as an icelike substance composed of water molecules forming a rigid lattice of cages that trap a guest molecule (Sloan, 2003). The predominant guest

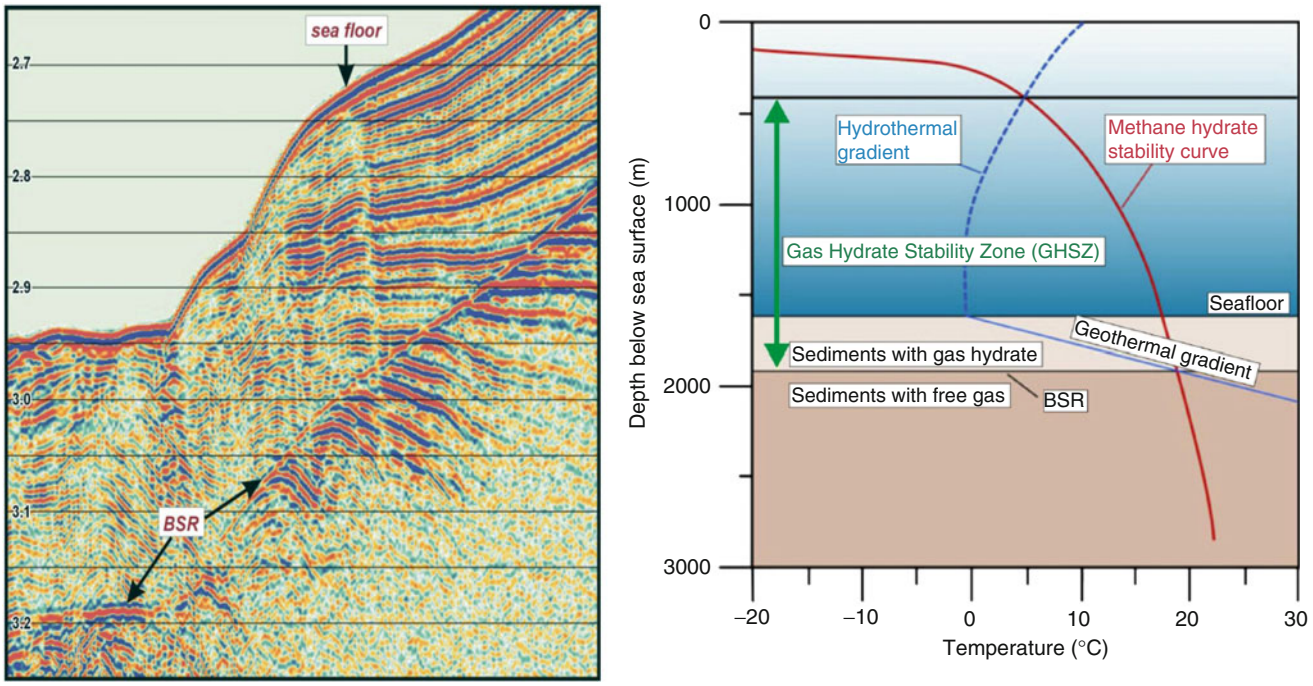

Bottom Simulating Seismic Reflectors (BSR), Figure 2 Reflection seismic profile of a hydrate/free gas BSR that follows the sub-bottom depths and coincides with the predicted depth of the base of the gas hydrate stability zone (schematic diagram, *right*). The gas hydrate stability zone is shown as a function of water temperature, pressure, and geothermal gradient.

molecule in the submarine environment is methane, but also hydrates containing high-order hydrocarbons, carbon dioxide, hydrogen sulfide, or other gas may exist. Gas hydrates occur naturally in the pore space of different types of marine sediments, where appropriate high-pressure and low-temperature conditions exist and there is an adequate supply of gas and water (Figure 2) (Kvenvolden, 1993; Rempel and Buffett, 1997; Sloan, 2003). Those requirements confine marine gas hydrates to the upper few hundred meters of the shallow geosphere of continental margins, where biogenic processes produce sufficient amounts of methane gas. The gas hydrate-related BSR detected on marine seismic reflection data commonly corresponds to the base of the gas hydrate stability zone (GHSZ, Figure 2). It is the result of an acoustic impedance contrast between hydrate-bearing sediments (increase in compressional-wave velocity) and free gas trapped in the sediments underneath (decrease in velocity) gas hydrates (Hyndman and Spence, 1992; Bünz et al., 2003). As a consequence, the hydrate-related BSR has reversed polarity (compared to the seafloor reflection) and is often accompanied by high-reflection amplitudes. The gassy sediments beneath the hydrate-bearing sediments also show on the instantaneous frequency attribute as the free gas predominantly attenuates the high-frequency content of the seismic signal (Berndt et al., 2004).

The BSR shows not always as a reflection proper because gas beneath the hydrated sediments accumulates only in places where rock properties of the host rock have high enough permeability. The seismic reflection shows higher amplitudes preferentially in areas where appreciable amounts of gas accumulate beneath the GHSZ (Figs. 3 and 4). Thus, whether the BSR is a true reflection in its own right on the seismic data is mainly the result of the frequency bandwidth of the acquisition system (Wood et al., 2002). High-frequency seismic acquisition systems often image gas accumulations along layers. The BSR is then identified as the envelope of amplitude increases that crosscuts stratigraphic boundaries (Figs. 2, 3, and 4). The BSR generally lies shallower than a diagenetic BSR, has a smaller areal extent, and might often show in patches over a larger area.

Assumptions on the possible presence of gas hydrate-/free gas-related BSRs along continental margins are based largely on modeling the GHSZ (Figure 2) (Dickens and Quinby-Hunt, 1997; Zatsepina and Buffett, 1998). The modeling and thus the theoretical potential for the existence of a BSR are mainly based on water depth (pressure), seafloor temperature, and the geothermal

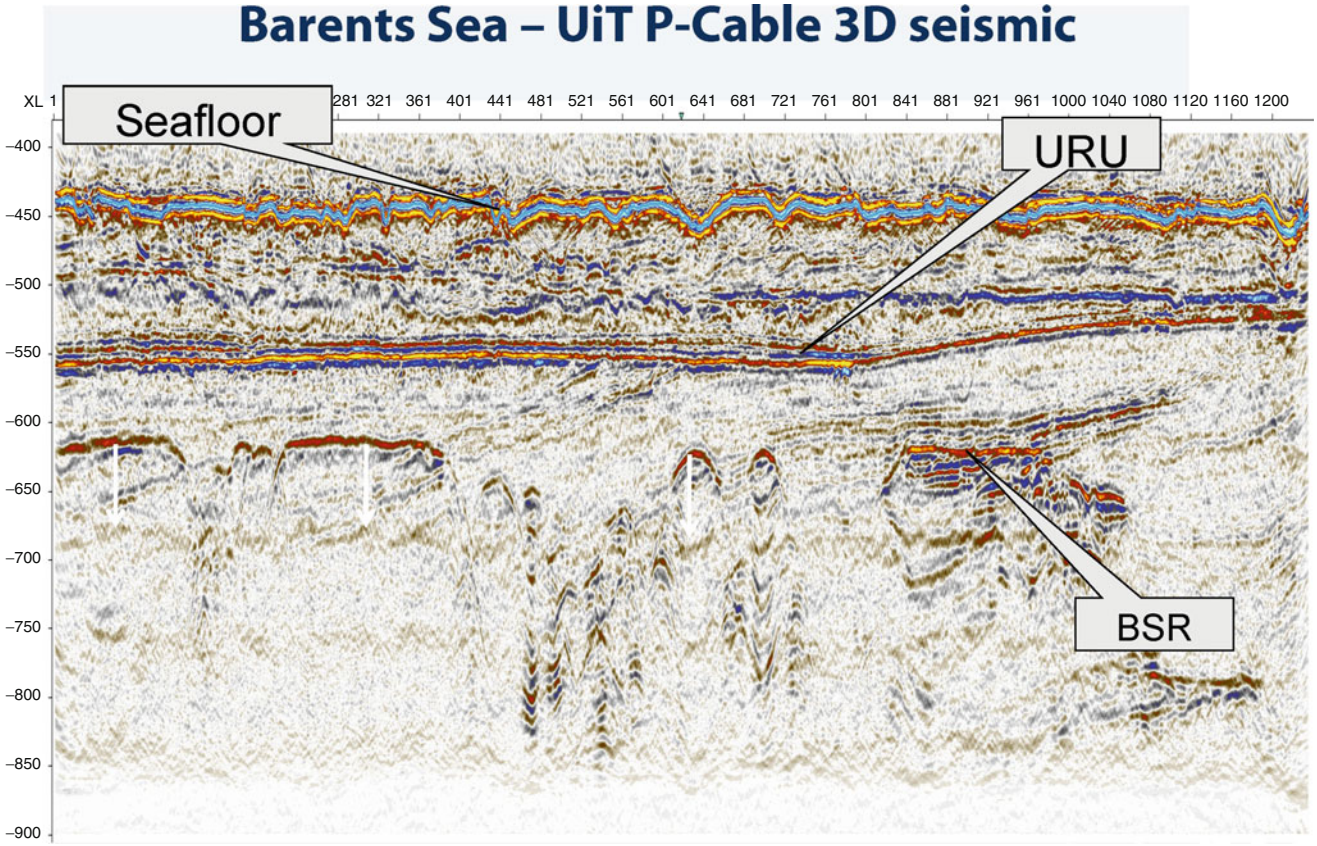

Bottom Simulating Seismic Reflectors (BSR), Figure 3 High-resolution 3D P-Cable seismic data showing higher amplitudes beneath the upper regional unconformity (*URU*) in the SW-Barents Sea. This high-amplitude reflection crosscuts sedimentary reflections with reversed polarity and is interpreted as BSR at the base of the GHSZ.

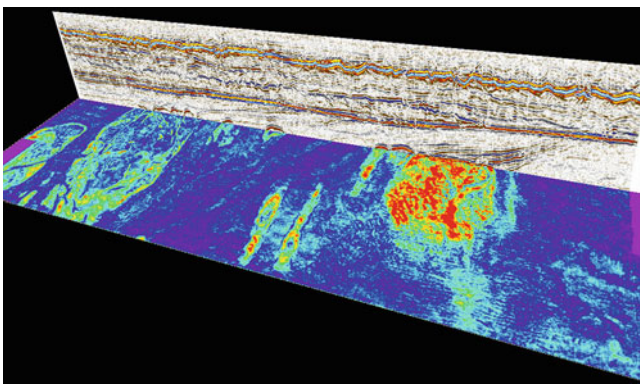

Bottom Simulating Seismic Reflectors (BSR), Figure 4 High-resolution 3D P-Cable seismic data showing higher amplitudes preferentially in areas where appreciable amounts of gas accumulate beneath the GHSZ.

gradient (Figure 2). As these parameters are largely controlled by water depth from the shelf to the deep sea, the methane hydrate BSR shows two pinch-out zones, one at the shallow water depth where pressure becomes too low for hydrates to be stable and one toward the mid-ocean ridge where heat flow becomes too high. Thus, if one describes these two end members, one may still use the terminology BSR but should be clear that the BSR does not parallel the seafloor.

Seismic character of BSRs

BSRs related to hydrate/free gas phase transitions can be distinguished from opal-A/opal-CT phase transitions based on their phase polarity. While diagenetic BSRs have the same positive phase as the seafloor reflection (Figure 1), the hydrate/free gas BSRs show a phase reversal (Figure 2). This reversed polarity is due to the negative impedance contrast between hydrated sediments above (higher density and velocity) and gas-saturated sediments below (Hyndman and Spence, 1992). However, caution is necessary if the phase of the BSR is the only criterion used. Gas trapped beneath a diagenetic BSR may also result in a phase reversal. As a consequence one should use several criteria such as instantaneous frequency, phase reversal, and GHSZ modeling to predict the BSR depth. Frequencies are useful as additional criteria for gas hydrate BSRs. A shift from higher frequencies in the gas

hydrate zone to lower frequencies in the free gas zone (Berndt et al., 2004) beneath the BSR may be used.

Dynamics of BSRs

Both the diagenetic- and the hydrate-related BSR may be used to evaluate the thermal state or reconstruct the thermal development of a sedimentary basin (Grevemeyer and Villinger, 2001; Nouzé et al., 2009). Particularly, the hydrate-related BSR is widely used as a proxy for heat flow in marine sediments. On a small scale, BSR-derived heat flow changes may often be associated with structures that focus warm fluids from deep sediments like mud volcanoes (Depreiter et al., 2005) or chimneys (Rajan et al., 2013). In such instance, the BSR may not mimic the seafloor if lateral variations in heat flow or changes in gas compositions exist. Generally, an increase in heat flow causes a shoaling of a BSR, whereas an increase of higher-order hydrocarbons causes a deepening. Hence, the depth of the BSR may vary greatly as, for example, in the Barents Sea depending on the contribution and thus the amount of thermogenic gases migrating into the GHSZ (Chand et al., 2008; Rajan et al., 2013).

More recently, BSR observations and hydrate stability zone modeling of the upper pinch-out zone on continental margins have been used to assess past and contemporary changes in hydrate stability through warming of ocean bottom water (Vogt and Jung, 2002; Mienert et al., 2005; Biastoch et al., 2011; Ferré et al., 2012; Phrampus and Hornbach, 2012).

Inferred former positions of a BSR are often referred to as paleo-BSR. One of the best examples for a paleo-BSR can be found on the Blake Ridge, approx. 450 km offshore Georgia on the East Coast of the United States (Hornbach et al., 2003). This BSR formed when erosion by strong contour currents on the eastern flank of the Blake Ridge removed the top sediments of a hydrated formation causing an adjustment of the hydrate/free gas boundary by moving it deeper. The free gas layer beneath the former BSR crystallized into a newly formed concentrated layer of hydrates causing both a density and velocity increase. Beneath this paleo-BSR, the new BSR formed with free gas underneath the base of the gas hydrate stability zone (BGHSZ). Though the timing of the readjustment is unknown, it presents one good example for the dynamic behavior (in this case deepening) of a BSR due to erosion of sediments and a drop in seafloor temperature.

Summary and conclusions

Bottom-simulating reflectors (BSRs) occur in a wide range of sediments in the world oceans. Such creation of BSRs involves the existence of free gas and water in the pore space of sediments under low temperature and high pressure, forming hydrates beneath the ocean floor. The depth of the BSR defines the base of the gas hydrate stability zone (BGHSZ) under which free gas accumulates. Free gas becomes trapped beneath the hydrate-charged layer causing a distinct impedance contrast and a seismic reflection of reversed (negative) polarity if compared to the seafloor. The GHSZ depends on temperature and pressure and to a lesser degree on salinity and gas composition (thermogenic, biogenic). The thickness of the GHSZ decreases toward the upper continental margins (lower pressure) and sedimented ocean ridges (higher temperature). The second type of BSRs concentrates in regions of siliceous ocean sediments. Here, increases in temperature with burial depth result in dissolution of siliceous skeletons, which in turn creates an interface with higher porosity and permeability above and lower values beneath the interface. If the contrast becomes large enough, a seismic reflector occurs but with positive polarity (no phase reversal). As a consequence, diagenetic BSRs occur commonly deeper, show no phase reversal, and exist over large areas at the opal-A/opal-CT interface in ocean sediments.

Bibliography

Berndt, C., Bünz, S., Clayton, T., Mienert, J., and Saunders, M., 2004. Seismic character of bottom simulating reflectors: examples from the mid-Norwegian margin. *Marine and Petroleum Geology*, **21**, 723–733.

Biastoch, A., Treude, T., Rüpke, L. H., Riebesell, U., Roth, C., Burwicz, E. B., Park, W., Latif, M., Böning, C. W., Madec, G., and Wallmann, K., 2011. Rising Arctic Ocean temperatures cause gas hydrate destabilization and ocean acidification. *Geophysical Research Letters*, **38**, L08602.

Brekke, H., 2000. The tectonic evolution of the Norwegian Sea continental margin with emphasis on the Vøring and More basins. In Nottvedt, A. (ed.), *Dynamics of the Norwegian Margin*. Geological Society of London Special Publication 167. London: Geological Society, pp. 327–378.

Bünz, S., Mienert, J., and Berndt, C., 2003. Geological controls on the Storegga gas-hydrate system of the mid-Norwegian continental margin. *Earth and Planetary Science Letters*, **209**(3–4), 291–307.

Cartwright, J. A., and Dewhurst, D. N., 1998. Layer-bound compaction faults in fine-grained sediments. *Bulletin of the Geological Society of America*, **110**(10), 1242–1257.

Chand, S., Mienert, J., Andreassem, K., Knies, J., Plassen, L., and Fotland, B., 2008. Gas hydrate stability zone modelling in areas of salt tectonics and pockmarks of the Barents Sea suggest an active hydrocarbon venting system. *Marine and Petroleum Geology*, **25**, 625–636.

Davies, R. J., and Cartwright, J. A., 2002. A fossilized opal-A to opal C/T transformation on the northeast Atlantic margin: support for a significantly elevated paleogeothermal gradient during the Neogene? *Basin Research*, **14**, 467–486.

Depreiter, D., Poort, J., Van Rensbergen, P., and Henriet, J. P., 2005. Geophysical evidence of gas hydrates in shallow submarine mud volcanoes on the Moroccan margin. *Journal of Geophysical Research*, **110**, B10103, doi:10.1029/2005JB003622.

Dickens, G. R., and Quinby-Hunt, M. S., 1997. Methane hydrate stability in pore water: a simple theoretical approach for geophysical applications. *Journal of Geophysical Research*, **102**, 773–783.

Ferré, B., Mienert, J., and Feseker, T., 2012. Ocean temperature variability for the past 60 years on the Norwegian-Svalbard margin influences gas hydrate stability on human time scales. *Journal of Geophysical Research, Oceans*, **117**, C10017.

Grevemeyer, I., and Villinger, H., 2001. Gas hydrate stability and the assessment of heat flow through continental margins. *Geophysical Journal International*, **145**, 647–660.

Hein, J. R., Scholl, D. W., Barron, J. A., Jones, M. G., and Miller, J. J., 1978. Diagenesis of Late Cenozoic diatomaceous deposits and formation of the bottom simulating reflector in the southern Bering Sea. *Sedimentology*, **25**, 155–181.
Hesse, R., 1989. Silica diagenesis: origin of inorganic and replacement cherts. *Earth-Science Reviews*, **26**, 253–284.
Holland, H. D., and Turekian, K. K., 2003. *Treatise on Geochemistry*. Elsevier Pergamon, Elsevier Ltd. The Boulevard, Langford Lane, Kidlington, Oxford, QX5 IGB, UK, ISBN 978-0-08-043751-4.
Hornbach, M. J., Holbrook, W. S., Gorman, A. R., Hackwith, K. L., Lizarralde, D., and Pecher, I., 2003. Direct seismic detection of methane hydrate on the Blake Ridge. *Geophysics*, **68**(1), 92–100.
Hurd, D. C., and Birdwhistell, S., 1983. On producing a more general model for biogenic silica dissolution. *American Journal of Science*, **283**, 1–28.
Hyndman, R. D., and Spence, G. D., 1992. A seismic study of methane hydrate marine bottom simulating reflectors. *Journal of Geophysical Research – Solid Earth*, **97**, 6683–6698.
Knauth, L. P., 1994. Petrogenesis of chert. *Reviews of Mineralogy*, **29**, 233–258.
Kotelnikova, S., 2002. Microbial production and oxidation of methane in deep subsurface. *Earth-Science Reviews*, **58**, 367–395.
Kvenvolden, K. A., 1993. Gas hydrates – geological perspective and global change. *Reviews of Geophysics*, **31**, 173–187.
Mienert, J., Vanneste, M., Bunz, S., Andreassen, K., Haflidason, H., and Sejrup, H. P., 2005. Ocean warming and gas hydrate stability on the mid-Norwegian margin at the Storegga Slide. *Marine and Petroleum Geology*, **22**, 233–244.
Nouzé, H., Cosquer, E., Collot, J., Foucher, L. P., Klingelhoefer, F., Lafoy, Y., and Géli, L., 2009. Geophysical characterization of bottom simulating reflectors in the Fairway Basin (off New Caledonia, Southwest Pacific), based on high resolution seismic profiles and heat flow data. *Marine Geology*, **266**(1–4), 80–90.
Phrampus, B. J., and Hornbach, M. J., 2012. Recent changes to the Gulf Stream causing widespread gas hydrate destabilization. *Nature*, **490**(7421), 527–530.
Rajan, A., Bünz, S., Mienert, J., and Smith, A. J., 2013. Gas hydrate in petroleum provinces of the SW-Barents Sea. *Marine and Petroleum Geology*, **46**, 92–106.
Rempel, A. W., and Buffett, B. A., 1997. Formation and accumulation of gas hydrate in porous media. *Journal of Geophysical Research*, **102**, 10151–10164.
Shipley, T. H., Houston, M. H., Buffler, R. T., Shaub, F. J., McMillen, K. J., Ladd, J. W., and Worzel, J. L., 1979. Seismic reflection evidence for the widespread occurrence of possible gas-hydrate horizons on continental slopes and rises. *American Association of Petroleum Geologists Bulletin*, **63**, 2204–2213.
Sloan, D. R., 2003. Fundamental principles and applications of natural gas hydrates. *Nature*, **426**, 353–359.
Tribble, J. S., Mackenzie, F. T., Urmos, J., O'Brien, D. K., and Manghnani, M. H., 1992. Effects of biogenic silica on acoustic and physical properties of clay-rich marine sediments. *American Association of Petroleum Geologists Bulletin*, **76**, 792–804.
Vogt, P. R., and Jung, W. Y., 2002. Holocene mass wasting on upper non-Polar continental slopes – due to post-Glacial ocean warming and hydrate dissociation? *Geophysical Research Letters*, **29**, 55-1–55-4.
Wood, W. T., Gettrust, J. F., Chapman, N. R., Spence, G. D., and Hyndman, R. D., 2002. Decreased stability of methane hydrates in marine sediments owing to phase-boundary roughness. *Nature*, **420**, 656–660.
Zatsepina, O. Y., and Buffett, B. A., 1998. Thermodynamic conditions for the stability of gas hydrate in the seafloor. *Journal of Geophysical Research*, **103**, 24127–24139.

Cross-references

Cold Seeps
Deep-sea Sediments
Marine Gas Hydrates
Methane in Marine Sediments
Silica

BOTTOM-BOUNDARY LAYER

Wenyan Zhang
MARUM-Center for Marine Environmental Sciences, University of Bremen, Bremen, Germany

Definition

In marine geosciences, the bottom boundary layer (BBL) refers to a layer of flow in the immediate vicinity of the solid sea bottom where the effects of viscosity are significant in determining the characteristics of the flow. The BBL was first discovered by Prandtl (1905) in aerodynamics and subsequently applied to other fluids moving on the surface of a solid body.

Starting upwards from the sea bed, the total thickness of the BBL is defined as the distance above the bottom at which the mean flow velocity equals to 0.99 U_∞, where U_∞ is the free-stream velocity of a layer that is in a geostrophic balance overlying the BBL. On top of the geostrophically balanced layer is a surface layer subjected to wind-wave mixing. When both the bottom micro-topography is uniform and the overlying flow is steady, the BBL can be easily quantified from the vertical flow structure. Various ways exist to estimate the thickness δ of the BBL under neutral conditions (e.g., Grant and Madsen, 1986; Nielsen, 1992). In general, the BBL thickness at continental margins is at the order of 5–50 m.

Theoretically the BBL can be classified into three different sub-layers:

(1) A thin inner layer just above the bottom where turbulence is inhibited by the presence of the solid boundary. The flow is controlled by molecular viscosity and the shear stress is consistent with the bottom shear stress.
(2) An outer layer where turbulence shear dominates and viscous shear can be neglected.
(3) A transitional layer where both the viscous shear and the turbulence shear are important.

As the shear stress is almost constant and fulfills Newton's law of viscosity in the inner layer, flow velocity can thus be approximated by a linear form. However, this only applies to a hydraulically smooth bottom where bed roughness is too small to affect the velocity distribution. In hydraulically rough bottom, bed roughness is large enough to produce eddies close to the bottom and the inner layer may not be detectable. Upwards from the inner layer, the importance of molecular viscous decreases and turbulence gradually dominates the flow. Mean flow velocity in this transitional layer obeys the law of the wall and can be

approximated by a logarithmic function. The outer turbulent layer takes up a majority (80–90 %) of the BBL. Flow characteristics of this layer mainly depend on the velocity difference with the external free flow (i.e., velocity defect) and the overall scale of the boundary layer.

Wind waves affect the BBL by imposing a wave boundary layer wherever the water depth is less than half of the wave length. The wave-induced oscillatory water motion is affected by the sea bottom within the wave boundary layer.

However, in a natural continental shelf, any definition of the BBL structure is not straightforward due to the influences of many factors (e.g., density stratification, internal waves, seabed topography). A practical indicator for the BBL is a thermohaline pycnocline observed in the water column (e.g., Stips et al., 1998; Perlin et al., 2005). Just above the sea bottom, there is a homogenous layer of temperature, salinity, and density, which indicates the inner layer and the transitional layer.

Bibliography

Grant, W. D., and Madsen, O. S., 1986. The continental-shelf bottom boundary layer. *Annual Review of Fluid Mechanics*, **18**, 265–305.

Nielsen, P., 1992. Coastal bottom boundary layers and sediment transport. In Series Editor-in-Chief Liu, Philip L-F. (ed.), *Advanced Series on Ocean Engineering*. World Scientific Publishing Co. Pte. Ltd., Singapore, Vol. 4.

Perlin, A., Moum, J. N., and Klymak, J. M., 2005. Response of the bottom boundary layer over a sloping shelf to variations in alongshore wind. *Journal of Geophysical Research*, **110**, C10S09, doi:10.1029/2004JC002500.

Prandtl, L., 1905. *Verhandlungen des dritten internationalen Mathematiker-Kongresses in Heidelberg 1904*, Krazer, A. (ed.), Leipzig: Teubner, p. 484. English trans. Ackroyd, J. A. K., Axcell, B. P., Ruban, A. I. (eds.) 2001. *Early Developments of Modern Aerodynamics*. Oxford: Butterworth-Heinemann, p. 77.

Stips, A., Prandke, H., and Neumann, T., 1998. The structure and dynamics of the Bottom Boundary Layer in shallow sea areas without tidal influence: an experimental approach. *Progress in Oceanography*, **41**, 383–453.

Cross-references

Sediment Dynamics
Sediment Transport Models

BOUMA SEQUENCE

Thierry Mulder[1] and Heiko Hüneke[2]
[1]University of Bordeaux, Talence, France
[2]Institute of Geography and Geology, Ernst Moritz Arndt University, Greifswald, Germany

The Bouma sequence (named after Arnold H. Bouma, 1932–2011) is a characteristic set of sedimentary structures typically preserved within positively graded sand or silt-mud couplets. From base to top, Bouma (1962) differentiated the following intervals above an erosion surface or sharp boundary: (Ta) massive to graded sand, (Tb) plane-parallel laminated sand, (Tc) cross-laminated sand and silt, (Td) parallel-laminated sand to silt, and (Te) laminated to homogeneous mud (Figure 1). Because of nonuniform grain size distribution and flow transformations (Fisher, 1983), the complete sequence is rare. Turbidite beds represent the typical deposit of low-concentration turbidity flows and related non-cohesive density flows.

The Bouma sequence is the first model of sediment-laden gravity flows and represents the first predictive model in sedimentology. It is a facies model of combined suspension fallout and traction deposition by a bipartite density flow (see Mulder, 2011, for details). The successive divisions with typical sedimentary structures display a bottom-to-top decline in energy consistent with the grading.

The basal surface of many turbidites, i.e., the lower bounding surface of Ta, commonly displays erosional features produced by turbulent scouring (Lanteaume et al., 1967).

Turbidity flows commonly develop from stratified density flows with a strong vertical velocity gradient. Within such bipartite flows (basal laminar flow and a top turbulent flow), the high particle concentration of its basal parts hinders suspension fallout (Mulder, 2011). Consequently, a poorly graded Ta division can be interpreted as being deposited from a concentrated-flow basal part. Rapid deposition and resulting unstable initial grain packing are also indicated by the common occurrence of water-escape structures such as dish or pillar structures or dewatering pipes.

The Bouma divisions Tb to Te record the passage of the flow body with a fully turbulent regime and reflect flow deceleration (Walker, 1965). The parallel lamination (Tb division) results from plane-bed transport of sand in the upper flow regime. The ripple cross-lamination (Tc division) reflects settling of sand and silt from suspension while lower-flow-regime current ripples migrate on the seabed. Climbing-ripple cross-lamination and convolute lamination would indicate rapid fallout and short-lived liquefaction, respectively. The Tc division is the most common structure in turbidite beds because ripples are the easiest structures to form for a given grain size and velocity/flow energy.

The uppermost divisions (Td and Te) are mainly products of settling from suspension. The pelitic top (Te division) represents the interaction of ongoing pelagic production with the fine terrigenous particle fallout from the turbulent tail of the flow.

Bouma Sequence, Figure 1 Well-developed Bouma sequence (divisions Ta to Te from base to top) in a turbidite bed of the Carboniferous Crackington Formation at the sea cliff near Crackington Haven, Cornwall, England.

Bibliography

Bouma, A. H., 1962. *Sedimentology of Some Flysch Deposits. A Graphic Approach to Facies Interpretation*. Amsterdam: Elsevier.

Fisher, R. V., 1983. Flow transformations in sediment gravity flows. *Geology*, **11**, 273–274.

Lanteaume, M., Beaudoin, B., and Campredon, R., 1967. *Figures sédimentaires du flysch 'Grès d'Annot' du synclinal de Peira-Cava*. Paris: Editions du CNRS.

Mulder, T., 2011. Gravity processes on continental slope, rise and abyssal plains. In Hüneke, H., and Mulder, T. (eds.), *Deep-Sea Sediments*. Amsterdam: Elsevier, pp. 25–148.

Walker, R. G., 1965. The origin and significance of internal sedimentary structures of turbidites. *Proceedings of the Yorkshire Geological Society*, **35**, 1–32.

Cross-references

Deep-sea Fans
Turbidites